# The BOLD Signal is more than a Brain Activation Index

# Das BOLD Signal ist mehr als ein Maß für Hirnaktivierung

Doctoral thesis for a doctoral degree

at the Graduate School of Life Sciences,

Julius-Maximilians-Universität Würzburg,

Section Neuroscience

submitted by

Atae Akhrif, Dipl. Ing. (FH)

Würzburg, 2019

Submitted on: ……..

Office stamp

Members of the *Promotionskomitee*:

Chairperson: Prof. Dr. med. Michael Sendtner

Primary Supervisor: Prof. Dr. med. Marcel Romanos

Supervisor (Second): Prof. Dr. Dr. Katharina Domschke

Supervisor (Third): PD. Dr. Angelika Schmitt-Böhrer

Date of Public Defence: ……

Date of Receipt of Certificates: ……

# Table of Content

# List of Figures



# List of Tables

# Abstract

In the recent years, translational studies comparing imaging data of animals and humans have gained increasing scientific interests with crucial findings stemming from both, human and animal work. In order to harmonize statistical analyses of data from different species and to optimize the transfer of knowledge between them, shared data acquisition protocols and combined statistical approaches have to be identified. Following this idea, methods of data analysis, which have until now mainly been used to model neural responses of electrophysiological recordings from rodent data, were applied on human hemodynamic responses (i.e. Blood-Oxygen-Level-Dependent BOLD signal) as measured via functional magnetic resonance imaging (fMRI).

At the example of two attention and impulsivity networks, timing dynamics and amplitude of the fMRI signal were determined (study 1). Study 2 described the same parameters frequency-specifically, and in study 3, the complexity of neural processing was quantified in terms of fractality. Determined parameters were compared with regard to the subjects' task performance / impulsivity to validate findings with regard to reports of the current scientific debate.

In a general discussion, overlapping as well as additional information of methodological approaches were discussed with regard to its potential for biomarkers in the context of neuropsychiatric disorders.

# Zusammenfassung

In den letzten Jahren haben translationale Studien, in denen Befunde von Tieren und Menschen direkt verglichen werden, zunehmend an wissenschaftlichem Interesse gewonnen. Um statistische Analysen von Daten verschiedener Spezies zu harmonisieren und somit den Wissenstransfer zu optimieren, müssen gemeinsame Datenerfassungsprotokolle sowie kombinierte statistische Ansätze identifiziert werden. Diesem Gedanken folgend werden in dieser Arbeit Methoden der Datenanalyse, die bisher hauptsächlich zur Modellierung neuronaler Antworten aus elektrophysiologischer Aufzeichnungen bei Nagetierdaten verwendet wurden, auf hämodynamische Antworten (d.h. Blood-Oxygen-Level-Dependent BOLD-Signal), welche mittels funktionaler Magnetresonanztomo-graphie (fMRT) gemessen werden, im Menschen angewendet.

Am Beispiel zweier Aufmerksamkeits- und Impulsivitätsnetzwerke wurden der zeitliche Verlauf und Amplitude des fMRI-Signals bestimmt (Studie 1). In Studie 2 wurden die gleichen Parameter frequenzspezifisch ausgewertet, und in Studie 3 wurde die Komplexität neuronaler Verarbeitung anhand von Fraktalität quantifiziert. Die ermittelten Parameter wurden hinsichtlich der Task Performance / Impulsivität der Probanden verglichen, um die Ergebnisse im Kontext von Befunden aus der aktuellen wissenschaftlichen Debatte zu validieren.

In einer allgemeinen Diskussion wurden sowohl überlappende als auch zusätzliche Informationen zu methodischen Ansätzen hinsichtlich ihres Potenzials für Biomarker im Zusammenhang mit neuropsychiatrischen Erkrankungen diskutiert.

# General Introduction

*If people do not believe that mathematics is simple,*

*It is only, because they do not realize, how complicated life is.*

John von Neumann

In the recent years, translational studies comparing imaging data of animals and humans have gained increasing scientific interest with crucial findings stemming from both, human and animal work (e.g. Logothetis, Pauls, Augath, Trinath, & Oeltermann, 2001; Magri, Schridde, Murayama, Panzeri, & Logothetis, 2012). In order to harmonize statistical analyses of data from different species and to optimize the transfer of knowledge between them, shared data acquisition protocols and combined statistical approaches have to be identified. Following this idea, methods of data analyses, which have until now mainly been used to model neural responses of electrophysiological recordings from rodent data, will be applied on human hemodynamic responses (i.e. Blood-Oxygen-Level-Dependent BOLD signal) as measured via functional magnetic resonance imaging (fMRI).

fMRI is one of the most widely used techniques to address neural activation at rest as well as under task condition. The standard statistical approach relies on the general linear model (GLM), where the entire fMRI time course is split and locked to the onset time of a stimulus of a certain experimental condition. These condition-specific pieces are then grouped and averaged to identify those brain regions, which showed a significant activation in that condition. Thus, GLM is applied (i) to separate stimulus-induced brain activation from noise and (ii) to average brain activation to identify relevant over random brain activation (Friston et al., 1994; Monti, 2011).

In the context of fMRI, the analysis of the entire fMRI time course has been applied, e.g. for the analysis of functional connectivity using independent component analysis. Here, time courses of the whole brain are correlated with each other to identify whether an activation in a certain region A is related to a second region B (Vince Daniel Calhoun, Adali, Stevens, Kiehl, & Pekar, 2005; V. D. Calhoun & de Lacy, 2017). Regions can either be correlated (when activation in region A increases, activation in region B increases, too) or anti-correlated (when activation in region A increases, activation in region B decreases), as well as with a temporal delay (e.g. region A

increases, after 2 seconds region B increases). In addition, Region-of-Interest (ROI)-based approaches such as Dynamic Causal Modeling make use of regional fMRI time courses. Here, brain regions are selected based on *a priori* knowledge and the regional time courses in these regions are extracted. Effective connectivity is defined as the influence region A has on region B (Stephan et al., 2010), or region C has on the connectivity between region A and B (Stephan et al., 2008).

From animal research and especially electrophysiological recordings, the analysis of entire time series is much more frequent (wavelet transforms: Percival & Walden, 2006; spectral analysis: Priestley, 1981 etc.). The relation between electrophysiological recordings and BOLD response has been empirically proven by Logothetis and coworkers in numerous studies (Logothetis et al., 2001; Magri et al., 2012). For example, they found that local field potentials (LFP) reflect best hemodynamic responses and it is mainly the component of the gamma band (60–120 Hz) which correlated positively with fMRI data (Logothetis et al., 2001). Subsequent studies were able to differentiate between amplitude and timing characteristics the way the amplitude of the BOLD signal reliably reflected both the increases and decreases in gamma power. Timing dynamics of the BOLD signal, in turn, reflected activity in the beta band (18-28 Hz) (Magri et al., 2012), with a higher beta power corresponded to faster increases (slower decreases) of the BOLD signal, and reciprocally a lower beta power to faster decreases (slower increases) of the BOLD signal. In the cognitive domain, LFP neural oscillations in the gamma frequency band were proven to play a crucial role in the synchronization of neural firing (Brunet, Vinck, Bosman, Singer, & Fries, 2014) as well as in cognitive information processing and focused attention (Melloni et al., 2007). On the other hand, beta band oscillations have been associated with selective attention (e.g. Gao et al., 2017), where a decrease of activity reflected a state of increased processing capabilities (Neuper, Scherer, Wriessnegger, & Pfurtscheller, 2009).

## Applied Methodological Approaches

In this dissertation, three methodological approaches were presented, which addressed aspects of brain function beyond the conventional brain activation and neural connectivity approaches. All analyses referred to frequently used methods of the analysis of electrophysiological recordings in animals, however, are rarely used on fMRI time series to date. In detail, the following approaches were used:

(a) **Bayesian Adaptive regression splines (BARS)** is a highly effective smoothing algorithm, which allows, when applied to histogram-based neuronal firing data, an estimation of the *instantaneous* firing rate of a certain neuron

/ brain region (Sam Behseta & Kass, 2005; Kass, Ventura, & Cai, 2003; C. G. Kaufman, Ventura, & Kass, 2005). BARS use cubic splines (piecewise cubic polynomials) which are joined at selected points (in this dissertation, fMRI time points) called 'knots' (DiMatteo, Genovese, & Kass, 2001; Kass, Ventura, & Brown, 2005). These pieces are constrained so that the resulting curve is smooth and fits well the fluctuation of the neural response. Thus, in the fMRI context, BARS describe the fluctuations in amplitude and temporal dynamics of the BOLD signal over the course of the entire measurement. The resulting curve is described by estimating the expectation value of a certain event (e.g. neural firing, increase of the amplitude of the BOLD signal), which is written as λ at each time point t (λ(t)) and its fluctuation over the time course in terms of peaks and troughs.

(b) wavelet transforms addresses the rhythmic fluctuations in regional time courses in the time-frequency space. Different frequencies of the fMRI signal reflect specific levels of processing such as network integration, *long/short-range* coupling, response to external stimulation and frequency modulation (Hramov, Koronovskii, Makarov, Pavlov, & Sitnikova, 2015). Furthermore, in the frequency domain, spectral coherence is a well-established standard tool to analyze the linear relationship between two signals by determining the correlation between their spectra (Yaesoubi, Allen, Miller, & Calhoun, 2015). A high spectral coherence suggests the presence of a functional coupling. Using wavelet transforms in this work, fMRI signals were characterized in terms of energy density, i.e. the maximum in the stimulus- induced frequency band, its frequency F(t) and stability. Modulation features were the modulating frequency (Fmod) and its amplitude (MFmod). Spectral coherence was quantified in terms of mean percent duration of sustained coherence relative to scan time, averaged over the stimulus band (meanperc).

(c) fractal analysis of BOLD time series: Fractal structures possess the property that the whole structure consists of parts, which have the same pattern composition but at different scales and / or in different sizes [e.g. broccoli, the Koch snowflake, (Koch, 1904, 1906; B. Mandelbrot, 1967; B. B. Mandelbrot, 1983)]. Fractals can be found not only in static objects but also dynamic processes. This property of *self-similarity*, or in the temporal domain *scale invariance* (P. Ivanov et al., 2009; Nagy, Mukli, Herman, & Eke, 2017; Suckling, Wink, Bernard, Barnes, & Bullmore, 2008) means that both, rapidly occurring changes and slowly proceeding dynamics follow the same structure, or better, that measures of the patterns are independent of the sampling rate, used during data acquisition (Riley, Bonnette, Kuznetsov, Wallot, & Gao, 2012). Fractal patterns have been examined in many research fields including physiology (for a systematic review see Sen & McGill, 2018) and neuroscience (for review see Di Ieva, Esteban,

Grizzi, Klonowski, & Martin-Landrove, 2015; Di Ieva, Grizzi, Jelinek, Pellionisz, & Losa, 2014). Studies using electrophysiological recordings and fMRI time series predominantly applied the adaptive fractal analysis (AFA) including the determination of the *Hurst Exponent* $H$ (Riley et al., 2012).

All methodological approaches were performed on regional fMRI time courses from task-based and resting-state fMRI (rs-fMRI) measurements and were extracted from whole brain activation maps. To identify relevant network regions in task-based fMRI, brain activation, induced by an experimental paradigm, had to be revealed using

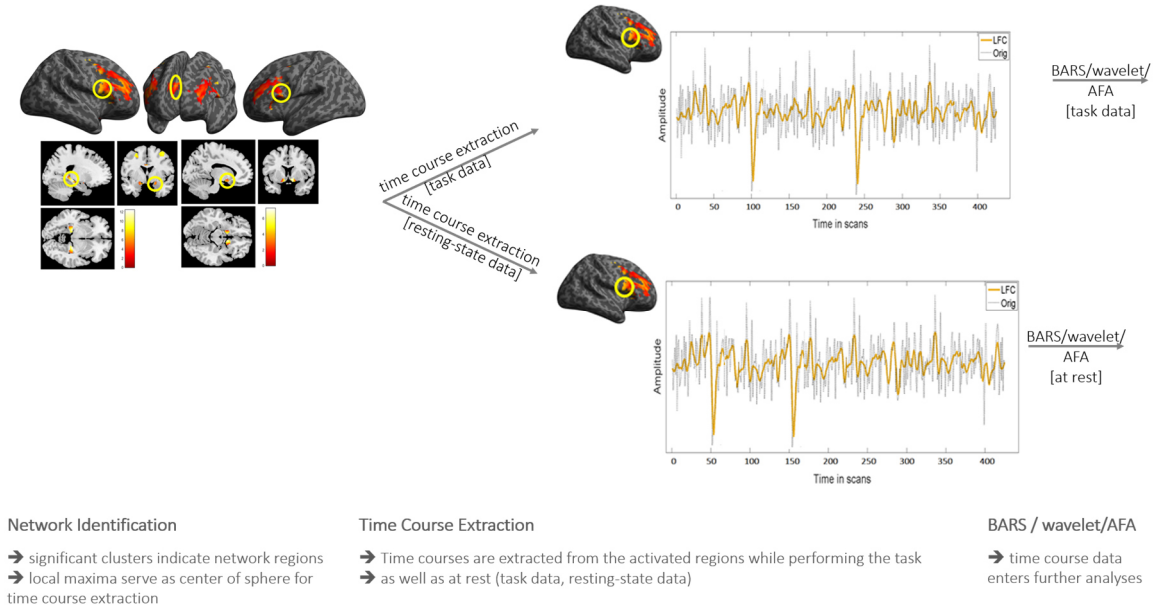


Figure 1 sketch of the procedure of time course extraction.
Note: BARS: Bayesian Adaptive Regression Splines, wavelet: wavelet transforms, AFA: adaptive fractal analysis

conventional whole brain fMRI analyses. Having identified exact localization of the significantly activated brain regions, maxima of the activation clusters were used as centers of the spherical masks, used for time course extraction. Time courses were extracted not only from fMRI task-data but also from resting-state data to compare brain response in these regions while performing a task and at rest. Resulting time courses were then used for BARS / wavelet transforms / AFA (for a workflow see **figure 1**).

## Examined Neural Networks

Data from two fMRI studies examining healthy adult participants was used (first published in S. Neufang et al., 2016; Neufang et al., 2015). In the first study, a sample of healthy volunteers underwent a task-fMRI measurement using the Attentional Network Task (ANT) by Fan et al. (2005) (Fan, McCandliss, Fossella, Flombaum, & Posner,

2005) (for a detailed description of the task see Appendix / Experimental Paradigms). Attentional processes as measurable by the ANT comprise the 'alerting' system, the 'orienting' system and the 'conflict' system (Posner & Petersen, 1990). The ANT has been used in numerous fMRI as well as EEG-studies showing most robust responses across the attention networks in the fronto-parietal regions as well as the striatum in terms of increased brain activation (Neufang et al., 2011; Neufang et al., 2015), as well as reflected by the event-related potential P300 in parietally-located electrodes (e.g. D. A. Kaufman, Bowers, Okun, Van Patten, & Perlstein, 2016). In addition, behavioral attention network scores showed significant correlation of the beta and gamma power in the fronto-central regions (Roh, Park, Shim, & Lee, 2016). Within a fronto-parieto-striatal attention network, the fronto-striatal loop has been described as a feedback loop to optimize response inhibition (Alexander, DeLong, & Strick, 1986; Vink et al., 2005) and form a top-down control, which means to ensure the ability to focus on the current task and not being distracted by further stimulations (Dosenbach, Fair, Cohen, Schlaggar, & Petersen, 2008). The parietal lobe, in turn, is understood as a bottom-up structure, perceiving task-relevant and irrelevant stimuli and then reporting these perceptions to higher order cortical structures such as the PFC (Neufang et al., 2011, 2014).

The experimental paradigm of the second study was the 5 choice serial reaction time task (5-CSRTT, Voon et al., 2014) examining waiting impulsivity (WI) (for a detailed description of the task see Appendix / Experimental Paradigms). In general, impulsivity is a personality trait, which spans from normal manifestations, e.g. in life time situations where decision making under time pressure is required (Burnett Heyes et al., 2012), to pathological presentations, mirroring the psychiatric symptoms of 'loss of control' and 'impulse control disorder' associated for example with attention deficit hyperactivity disorder (ADHD), (for a recent review see Hinshaw, 2017; e.g. Sebastian, Jacob, Lieb, & Tuscher, 2013). WI is defined as the tendency to premature responding, that is, to respond before target onset. Premature responses are assumed to arise because of the individual expecting a reward-related cue in combination with aspects of response inhibition. WI can be assessed using the 5-CSRTT. To date, the 5-CSRTT has mainly been employed in rodents (Robbins, 2002) with only a small number of human studies (Benson, Tiplady, & Scholey, 2019; Laurel S Morris et al., 2016; Nord et al., 2019; Voon et al., 2014; Worbe, Savulich, Voon, Fernandez-Egea, & Robbins, 2014). In electrophysiological studies in rodents, WI has been associated with the prefrontal cortex (PFC) including the anterior cingulate cortex (ACC) (Bubenzer-Busch et al., 2016), the dorsal and ventral prelimbic cortices (Balleine & O'doherty, 2010) (human homolog: dorsal cingulate cortex, Brodmann Area 32), and the infralimbic cortex (human homolog: ventromedial PFC (vmPFC), Brodmann

Area 25) interacting with mediotemporal structures such as the hippocampus (HC) and the amygdala (AMY), and the nucleus accumbens (NAcc) (Christopher D Chambers, Hugh Garavan, & Mark A Bellgrove, 2009; Jeffrey W Dalley, Barry J Everitt, & Trevor W Robbins, 2011). In humans, its associated functional network consists of the dorso-lateral PFC (dlPFC) and the vmPFC representing impulse control (Mechelmans et al., 2017), the reward-perception-related NAcc, the ACC for the cognitive evaluation of the reward and HC and AMY responsible for reward-based learning (J. W. Dalley, B. J. Everitt, & T. W. Robbins, 2011).

Impulsivity has been documented to have an effect on cognitive functions. For example, high impulsive healthy subjects showed reduced activation in right dlPFC while performing a decision making task (Deserno et al., 2015), bilaterally in the vmPFC during motor inhibition (Goya-Maldonado et al., 2010) as well as in the dlPFC and the HC in aggressive impulsive subjects (Sala et al., 2011). At rest, impulsivity affected functional connectivity from rs-fMRI in terms of less elaborated neural network architecture, e.g. lateral and medial PFC regions were isolated from reward associated NAcc (Davis et al., 2013), connectivity between the NAcc and the ACC as well as the ACC and the AMY (N. Li et al., 2013). The best examined structures of the WI network, to date, are the NAcc and the vmPFC with regard to their functional interaction. For example, Donnelly et al. examined rats while performing the 5-CSRTT and reported that gamma frequency (50–60Hz) in LFP oscillations transiently increased in the vmPFC and NAcc during the waiting period and after the performance of a correct response. The first finding was discussed to presumably reflect increasing top-down control demands over waiting time (Linnet, 2014) and the second finding being associated with the processing of reward (Linnet, 2014; Schultz, 2006). High impulsive rats (animals with high number of premature responses) showed reduced activity during the waiting period (Nicholas A Donnelly et al., 2014) predominantly in the vmPFC, hinting towards an impaired top-down control in high impulsive animals. In humans, a first fMRI study found a high overlap with reports from animal studies with regard to the underlying cognitive processes, brain regions associated with WI and the neural interplay between the NAcc and vmPFC, concluding that the 5-CSRTT is a promising tool for translational studies (S Neufang et al., 2016).

In both studies of this thesis, only data of healthy control subjects were analyzed to minimize data variation and to assure the pure basic science nature of this dissertation.

## Aims and Hypotheses

In this dissertation, we expected to find, that across all analyses, **BARS / Wavelet Transforms / AFA parameters dos reflect human neural processing at rest as well as under task condition, based on findings from animal studies and attention / impulsivity phenotype literature.**

In detail, in Study 1 subjects were divided by median split into good and bad performers ($n_{good}$=23, $n_{bad}$=24) based on the overall accuracy, defined as the proportion of correct trials from all trials. Good performers were assumed to present a significantly higher overall accuracy on the behavioral level in combination with a stronger frontal top-down control reflected by higher activation in fronto-striatal regions. Regarding the relation between brain activation and BARS, regions with a higher brain activation were supposed to present higher expectation values λ(t), reflecting a higher gamma power. On the other hand, regions of reduced brain activation were supposed to go along with stronger fluctuating expectation values λ(t), indicating stronger beta power.

In Studies 2 and 3, the impulsive phenotype was defined as high impulsive (highImp) versus low impulsive subjects (lowImp), based on the subjects' number of premature responses. If the number was ≥ 3, subjects were classified as highImp and if the number was <3 as lowImp. Threshold definition was adapted from Feja et al. (2014) in terms of the median value of premature responses across all subjects [range: 0–6 number of premature responses (Feja, Hayn, & Koch, 2014)].

It was hypothesized, that lowImp subjects were expected to present a higher stability in the vmPFC compared to highImp subjects, reflecting the stronger frontal top-down regulation, in combination with a more stable modulation in lowImp subjects, representing the more effective coupling between the NAcc and the vmPFC in lowImp compared to highImp. In contrast, highImp subjects were hypothesized to work with a higher energy in combination with deviation of the modulating frequency reflecting the more ineffective way of processing due to the imbalance between reward-driven NAcc and controlling vmPFC.

In AFA of study 3, a fractal nature of the WI network was assumed and that $H$ values of all network regions were close to 1. In addition, $H$ was hypothesized to be smaller at task compared to rest (Barnes, Bullmore, & Suckling, 2009; Churchill et al., 2016; Ciuciu, Varoquaux, Abry, Sadaghiani, & Kleinschmidt, 2012). Finally, a significant influence of impulsivity on $H$ was assumed in the PFC and the NAcc (Hahn et al., 2012; Wink, Bullmore, Barnes,

Bernard, & Suckling, 2008). In line with the previous studies (Gilden & Hancock, 2007; Hausdorff, 2007) a deviation from 1/f noise pronounced in highImp compared to lowImp subjects was expected.

Applying methodological approaches, which have until now mainly been used to model neural responses of electrophysiological recordings from rodent data, on human fMRI data facilitates the knowledge transfer between species and might open new ways to harmonize study designs across translational research.

Despite of wavelet transforms (Study 2), findings reported in this thesis have been published in the following publications:

Akhrif A, Geiger MJ, Romanos M, Domschke K, Neufang S (2017), Task Performance changes the amplitude and timing of the BOLD signal. *Transl Neurosci,* 8: 182-190. (Study 1)

Neufang S, Akhrif A, Hermann CG, Drepper C, Homola GA, Nowal J, Waider J, Schmitt AG, Lesch KP, Romanos M (2016). Serotonergic modulation of 'waiting impulsivity' is mediated by the impulsivity phenotype in humans. *Transl Psychiatry,* 6(11): e940. (Study 3)

Akhrif A, Romanos M, Domschke K, Schmitt-Boehrer A, Neufang S (2018). Fractal Analysis of BOLD Time Series in a Network Associated with Waiting Impulsivity. *Front Physiol.* 9:1378. (Study 3)

# Study 1: BARS, ANT Network

## Study 1- Introduction

BARS is a smoothing algorithm / curve fitting technique. In neuroscience it is used to smooth neural time courses, spike trains and tuning curves from neurophysiological recordings (S. Behseta & Chenouri, 2011; Ramezan, Marriott, & Chenouri, 2014; Taubman, Vaadia, Paz, & Chechik, 2013), as well as regional fMRI time courses (DiMatteo et al., 2001). The graphical data representation of peristimulus-time histograms (PSTH) of a data set, for example spike trains of a single neuron, is accumulated for all trials under a particular set of experimental conditions to show the firing rate varies over time. One reason the PSTH works well is that our eye is able to smooth the PSTH so that we see the temporal evolution of the firing rate. However, once we have articulated the goal of estimating the firing rate, it is possible to improve the PSTH by smoothing (Kass et al., 2003). Estimating the firing rate in this context means producing an estimate of the instantaneous firing rate, which we write as λ(t), at each time *t*, where *t* varies across a whole range of experimental values of interest. In other words, we are interested in estimating the curve described by λ(t) (Kass et al., 2003). BARS use cubic splines (piecewise cubic polynomials) which are joined at selected points called 'knots' (DiMatteo et al., 2001; Kass et al., 2005), with the number of knots and their locations being based on a posterior probability distribution. The expectation of the unknown function of time is then taken to be the fitted curve (Sam Behseta & Kass, 2005; Kass et al., 2003; C. G. Kaufman et al., 2005; Muniz-Terrera et al., 2016; Taubman et al., 2013). In this study, BARS describe the fluctuations of the amplitude of the BOLD signal over the course of the entire measurement. The resulting curve is described by estimating the expectation value of a certain event (e.g. neural firing, increase of the amplitude of the BOLD signal), which is written as λ at each time point t λ(t) and its fluctuation over the time course in terms of peaks and troughs. To prove that BARS on fMRI correspond to cell recordings, we performed: i) conventional analyses of brain activation patterns using GLM in terms of an external validation and, ii) task performance of an attention task which the volunteers had to perform in the MRI scanner for behavioral correlate / ecological validation.

Within the fronto-parieto-striatal attention network, brain activation patterns and λ(t) were determined. The group factor *task performance* was operationalized by splitting the subjects into groups of good and bad performers according to their overall accuracy. Group differences were addressed in brain activation maps and

expectation values λ(t). We expected to differentiate good performers from bad performers in terms of stronger frontal top-down control reflected by higher activation in the fronto-striatal regions. Regarding the relation between brain activation and BARS, we expected to find that regions with a higher brain activation presented higher expectation values λ(t), indicating higher gamma power. On the other hand, regions of reduced brain activation were supposed to go along with stronger fluctuating expectation values λ(t), hinting towards stronger beta power.

# Study 1-Methods

## Participants

Forty-seven participants (f=23, m=24; mean age: 25.43+2.7 years) were examined. This sample had previously been investigated for the genetic influence of brain activation patterns using GLM (Geiger et al., 2016; Neufang et al., 2015). Subjects were drawn from a large pool of healthy German subjects consecutively recruited at the Department of Psychiatry, University of Würzburg, Germany. All subjects were screened for the absence of current or life-time history of mental axis I disorders by experienced clinical psychologists or psychiatrists using the Mini International Neuropsychiatric Interview (MINI, Cathebras, Mosnier, Levy, Bouchou, & Rousset, 1994). Right-handedness was ascertained using the Edinburgh Handedness Inventory (EHI, Oldfield, 1971). The study was approved by the ethics committee of the Faculty of Medicine, University of Würzburg, Germany, and was conducted in accordance with the declaration of Helsinki in its latest version from 2008. Written informed consent was obtained from all subjects.

## BARS: Expectation value of a BOLD event

In general, BARS are used to address generalized nonparametric regression (curve-fitting) problems by assuming that a function f(x) is approximated by cubic splines, i.e. piecewise cubic polynomials, which are joined at 'knots'. A Bayesian Monte Carlo method searches through the space of possible numbers of knots and their locations and provides an optimally fitted curve. The resulting curve is a data-driven estimate of the expectation value of a certain event (e.g. neural firing, increase in MRI signal), which is written λ for each time t (Kass et al., 2003).

## BOLD event definition

As the amplitude of the BOLD signal correlates with the activity of the neurons located in the specific region, we picked the amplitude value as the event of interest. An event corresponded to a BOLD amplitude that exceeded a

certain threshold. Threshold definition in BARS is data-driven (DiMatteo et al., 2001; Kass et al., 2003; Taubman et al., 2013) or based on the natural scales (Muniz-Terrera et al., 2016). In order to find the right value for the threshold, 10% of the maximal value of the amplitude was taken and increased step wisely until a value was found to differentiate the amplitudes between experimental groups. In our case, a thirty per cent of its overall maximum value. In probability theory, stochastic sequences of event times are best modeled using the point processes models. The simplest and most important point process model is the Poisson process. A number of events within a time window, the number of events one would expect to happen during an interval of time, therefore follows the Poisson distributions. In its general form, a point process is modeled by specifying its conditional intensity, λ(t), which represents the infinitesimal rate at which events are expected to occur around a particular time t, conditional on the prior history of the point process prior to time *t*. For a non-parametric estimate of λ(t), we applied BARS to smooth the Peri Event Time Histogram (PETH) of MRI data to get the average ROI response of all subjects.

## Raster Plot and PETH

A raster plot marks the occurrence of an event along the X-axis with a tick mark indicating the time it happens (see **figure 2A**). It displays the trial response of a specific ROI. To get the average response of a task, this procedure is repeated several times on a single subject level or over several subjects. An average ROI response is captured by the PETH showing how the response varies across time (see **figure 2B**). For the Y-axis to indicate the conditional intensity, each bin event count is divided by both, the bin width and the number of trials on single subject level. The shape of a histogram, or a PETH, changes every time the bin size changes. To get accurate values and

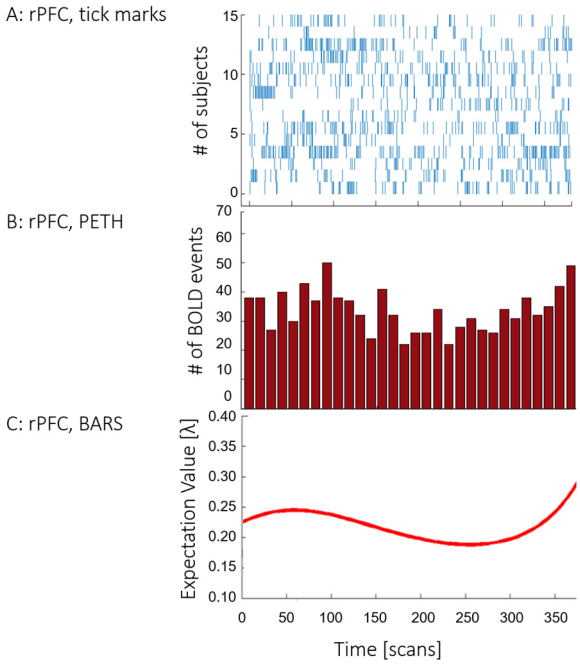


Figure 2 represents the analysis steps of BARS exemplarily for the task-related time course of the right prefrontal cortex (PFC). In (A), tick marks represent BOLD events of a specific subject (y-axis) at a certain time point (x-axis). In (B), tick marks have been converted into a Peri Event Time Histogram (PETH) by counting the overall number of BOLD events (y-axis) at a certain time bin (x-axis); BARS: Bayesian Adaptive Regression Splines. In (C), the smoothed PETH is shown.

comparable results across different trials, it is therefore important to look for an optimal size for the bin. The algorithm we used to calculate the optimal bin size was suggested by Shimazaki and Shimoto, 2007 (Shimazaki & Shinomoto, 2007). The resulting optimal bin number is 60 in our case. In the last step, we used the MATLAB version of the code published by Wallstrom et al. (2008) to smooth the PSTH (Wallstrom, Liebner, & Kass, 2008) (see **figure 2C**).

### BARS: Statistical Analysis

In order to statistically approach the spline, we determined: (a) $\lambda_{mean}$, i.e. the average expectation value of all bin-specific λ(t), (b) the range of λ($\lambda_{range}$) being the range from the maximum and minimum λ value, and (c) bin-specific λ(t), group comparisons were statistically addressed using the non-parametric Mann-Whitney Tests with performance group as an independent factor (good vs. bad performers) and $\lambda_{mean}$, $\lambda_{range}$ as well as bin-specific λ(t) as the dependent variables. Effects were considered significant when passing a statistical threshold of $p<.05$ FDR-corrected (Benjamini & Hochberg, 1995b). The characterization of the timing was based on the number of peaks and troughs and was reported descriptively.

## Study 1-Results

### GLM results

Across all subjects, we found a significantly activated bilateral fronto-parieto-striatal attention network with significant activation bilaterally within the superior parietal lobe (SPL, lSPL: x=-28, y=-56, z=54, Z=7.8; rSPL: x=-22, y=-60, z=62, Z=7.8), prefrontal cortex (PFC, l PFC: x=-40, y=10, z=34, Z=5.2, r PFC: x=38, y=6, z=32, Z=4.2) and pallidum (x=--18, y=-2, z=6, Z=4.6) were considered as ROIs and processed for BARS analysis (**figure 3**). The group comparison of the Main Effect of Attention Network Task revealed a significantly stronger activation bilaterally in the SPL, right PFC and striatum in good performers as compared to bad performers (lSPL: x=--22, y=-48, z=74, Z=3.2; rSPL: x=-34, y=-42, z=48, Z=3.0; rPFC: x=-32, y=26, z=36, Z=3.0). In contrast, bad performers activated stronger the left PFC (lPFC: x=-52, y=34, z=2, Z=3.1) (**figure 4A**).

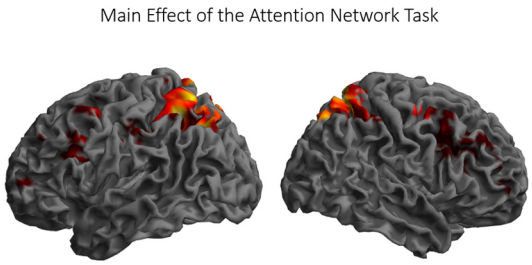


Figure 3 ANT brain activation
GLM brain activation results of the contrast Main effect of the Attention Network Task are presented.

## BARS results

Analyses revealed differences between performance groups bilaterally in the parietal regions, lPFC and striatum with regard to both the average expectation value $\lambda_{mean}$ and range $\lambda_{range}$. The $\lambda_{mean}$ was significantly higher in the lPFC of bad performers as compared to good performers (lSPL: $M_{good}$=0.35±0.07, $M_{bad}$=0.40±0.09, Z=1.9, n.s.; rSPL: $M_{good}$=0.36±0.10, $M_{bad}$=0.36±0.07, Z=0.1, n.s.; lPFC: $M_{good}$=0.34±0.07, $M_{bad}$=0.41±0.08, Z=3.0, p<.05; rPFC: $M_{good}$=0.33±0.05, $M_{bad}$=0.34±0.05, Z=0.5, n.s.; striatum: $M_{good}$=0.32±0.04, $M_{bad}$=0.37±0.09, Z=2.2, n.s.), whereas

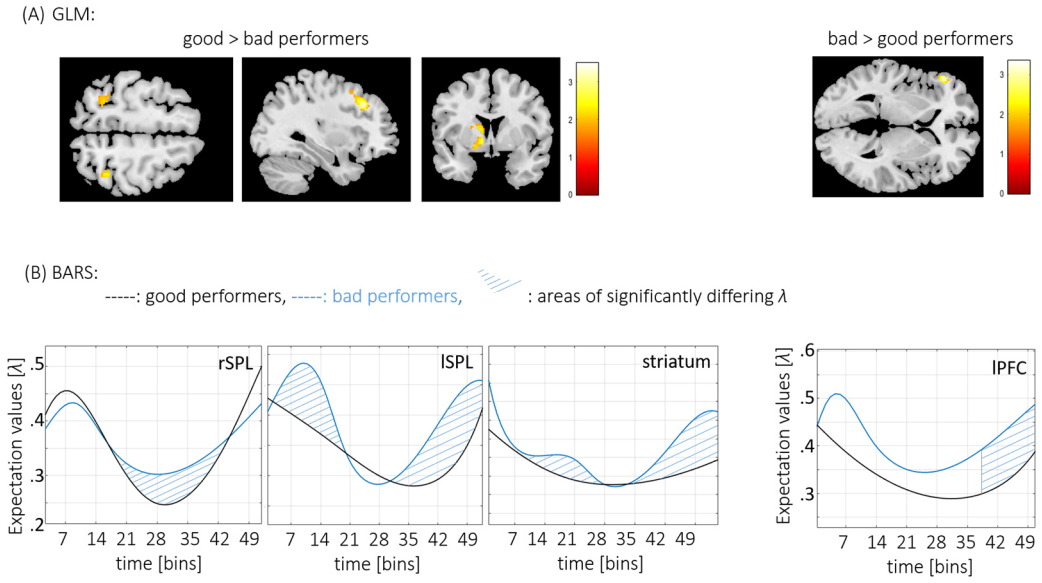


Figure 4 shows significant differences in BOLD events in the PFC.
In (A), performance-specific activation patterns are presented, (B) shows group-specific BARS for brain regions. The x-axis shows the timeline, indicated by bins, the y-axis represents the expectation value λ for a BOLD event.

they were similar in all other regions between performance groups. However, expectation values varied stronger in terms of higher $\lambda_{range}$ in the lSPL and striatal region in bad performers (lSPL: $range_{good}$=0.53, $range_{bad}$=0.61, Z=3.2, p<.05; rSPL: $range_{good}$=0.58, $range_{bad}$=0.47, Z=4.1, p<.01; lPFC: $range_{good}$=0.50, $range_{bad}$=0.46, Z=1.6, n.s.; rPFC: $range_{good}$=0.42, $range_{bad}$=0.44, Z=1.2, n.s.; striatum: $range_{good}$=0.16,

Table 1 Bin-specific expectation value

| region | bins | good | bad | Z |
|---|---|---|---|---|
| lSPL | 4-19 | .38(.02) | .47(.04) | 3.9** |
| | 31-51 | .32(.04) | .40(.04) | 4.3** |
| lPFC | 37-51 | .32(.03) | .37(.03) | 3.9** |
| rSPL | 17-44 | .25(.01) | .30(.01) | 4.0** |
| striatum | 11-28 | .24(.004) | .28(.001) | 3.4* |
| | 34-54 | .32(.01) | .38(.02) | 4.2** |

Note. lSPL: left superior parietal lobe, lPFC: left prefrontal cortex, rSPL: right superior parietal lobe, **: p<.01, FDR-corrected for multiple comparisons; *: p<.05, FDR-corrected for multiple comparisons.

$range_{bad}$=0.61, Z=21.9, p<.01) with no significant differences in the PFC region. In the rSPL, the range was higher in good performers as compared to bad performers. Finally, significant differences in bin-specific λ(t) values were found in all regions except for the rPFC, and also in the enhanced λ(t) values of bad performers as compared to good performers (**table 1**). Regarding the timing characteristics, good performers presented a flat U-shaped curve in all regions except for the right SPL. Bad performers, however, presented several fluctuations in the lSPL ($n_{good}$=1, $n_{bad}$=3), striatum ($n_{good}$=1, $n_{bad}$=4), and lPFC ($n_{good}$=1, $n_{bad}$=2) with significant deviations in the expectation value in several bins (**table 1, figure 4B**). In the rSPL ($n_{good}$=2, $n_{bad}$=2), fluctuations were more pronounced in good performers.

### Comparing GLM and BARS results

For the last step, we descriptively contrasted results from both analyses, GLM and BARS, to identify convergent and complementary information of both methodological approaches (see **table 2**). In doing so, we have identified three different patterns in reference to altered processing in bad performers: (a) stronger activation was combined with an enhanced average expectation values λ and bin-specific λ(t) values in the lPFC, (b) reduced activation was combined with enhanced fluctuation in terms of significantly enhanced range width of the expectation value λ and a higher number of peaks and troughs in the lSPL and striatum. In addition, some of the peaks λ increased significantly, and (c) reduced activation did not show significant differences with regard to λ (e.g. rPFC).

Table 2 Schematic overview of the relation between GLM and BARS parameters

| | Region | GLM | $\lambda_{mean}$ | $\lambda_{range}$ | Timing | $\lambda_{Bin\text{-}spec}$ |
|---|---|---|---|---|---|---|
| enhanced activation & enhanced λ in bad performers | | | | | | |
| | lPFC | ↑ | ↑ | n.s. | ↑ | ↑ |
| reduced activation & enhanced fluctuation in bad performers | | | | | | |
| | lSPL | ↓ | n.s. | ↑ | ↑ | ↑ |
| | stria | ↓ | n.s. | ↑ | ↑ | ↑ |
| similar curvature between performance groups | | | | | | |
| | rSPL | ↓ | n.s. | ↓ | n.s. | ↑ |
| | rPFC | ↓ | n.s. | n.s. | n.s. | n.s. |

Note. lSPL: left superior parietal lobe, lPFC: left prefrontal cortex, rSPL: right superior parietal lobe

## Study 1- Discussion

In this study, we investigated the influence of task performance on brain activation as well as the amplitude and timing of regional time course. We found that bad performers had reduced right fronto-striatal and bilateral

parietal activation in combination with enhanced lPFC activation. Additionally, across the entire time course, the lPFC region presented an enhanced BOLD signal amplitude in bad performers, hinting towards a compensatory enhanced gamma power in the lPFC. In the lSPL and striatum, reduced neural activation was accompanied by an enhanced range width of λ as well as stronger fluctuations during these time courses, suggesting a stronger beta power in bad performers within these regions. Splines in the rSPL and rPFC were similar between performance groups.

## Reduced right fronto-parietostriatal functioning and enhanced beta power

As introduced, the right frontal and bilateral parietal regions form the core of attention networks (Neufang et al., 2011; Peelen, Heslenfeld, & Theeuwes, 2004; Vossel, Thiel, & Fink, 2006), thus reduced activation in bad performers in these regions seemed plausible. The finding that reduced right fronto-parietal activation was related to an increased beta activity fits nicely into this context, with an increased beta activity hinting towards decreased processing abilities (Neuper et al., 2009). In detail, bad performers showed higher fluctuations mainly in parietal and striatal processing. Within a fronto-parietal attention network, parietal activity has been associated with bottom-up attentional orienting (Shomstein, Kravitz, & Behrmann, 2012), reflecting screening processes for stimuli (Corbetta & Shulman, 2002). Thus, continuous parietal processing in bad performers might reflect a constant parietal bottom-up processing and indicate a hyper aroused basal attentional state. With regard to beta oscillations in attention processing, firing rates in the pallidum exhibited a linear decrease in sequences of correct responses in a reward learning task in monkeys (Schechtman, Noblejas, Mizrahi, Dauber, & Bergman, 2016). In addition, beta oscillations in the human pallidum have been associated with motor control in healthy volunteers (Brown et al., 2002), as well as with alterations of the same in patients with Parkinson's Disease (Ahn, Zauber, Worth, & Rubchinsky, 2016; Muralidharan et al., 2016). In sum, a higher beta power in the parietal and striatal regions is associated with altered attentional performance and motor control. In combination with reduced brain activation in the right PFC, reflecting impaired top-down control, our findings revealed a plausible neural explanation for bad performance.

## Enhanced activation and gamma power in the left PFC

Brain activation as well as gamma activity in the PFC have predominantly been associated with cognitive control, top-down control and attention allocation (Buzsáki & Wang, 2012; Fries, Scheeringa, & Oostenveld, 2008; Rossi,

Pessoa, Desimone, & Ungerleider, 2009; Szczepanski et al., 2014). However, prefrontal recruitment in attentional networks induced by the ANT showed a right-hemispheric preference (Fan et al., 2005; Neufang et al., 2011), which seemed to be ontogenetically determined as developmental studies have reported that a reduction of lPFC activation with network maturation paralleled with performance improvement (Akhrif, Bajer, Wohlschläger, Konrad, & Neufang, 2013a; Durston et al., 2006). Thus, additional activation and increased gamma power in the contralateral PFC might reflect a compensatory mechanism to optimize performance. Alternatively, the lPFC plays a role in attentional processing of verbal learning (Breukelaar et al., 2017; Buckner & Koutstaal, 1998; Reynolds, Donaldson, Wagner, & Braver, 2004), auditory conflict processing (Weigl, Mecklinger, & Rosburg, 2016), and selective attention to lexical and speech sound (Alho et al., 2016; X. Li et al., 2003). Thus, it is possible that bad performers in our study used a verbal strategy before or during responding with a button press. A verbal indication of the direction would be mirrored by lPFC activation and gamma power and this might also explain the longer reaction time as verbalization might take some milliseconds.

# Study 2- Wavelets, WI Network

## Study 2- Introduction

Not only brain activation but also rhythmic fluctuations can reflect the functioning of brain regions. The most prominent method to represent time series in the frequency domain is the Fourier transform. Wavelet transforms, however, convert the signal into time-frequency space (e.g. see Bullmore et al., 2001; Meyer, 2003). Its visualization shows the distribution of energy densities over the time and frequency range with bright areas representing high energy density (**figure 5**). The energy density provides information about the local energy spectra at fixed time points.

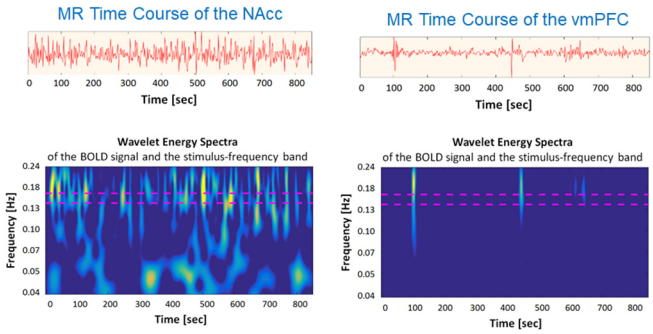


Figure 5 wavelet transforms of task-fMRI timecourses of NAcc and vmPFC. upper row: raw time course, lower row: wavelets transform. Pink lines indicate the frequency band of task-induced neural response. NAcc: nucleus accumbens, vmPFC: ventro-medial prefrontal cortex.

Frequencies in the brain can be divided into three main categories: Rhythmic fluctuations in slow frequency bands are responsible for network integration and *long range* coupling (Axmacher et al., 2010; Fell et al., 2001). Rhythmic fluctuations in the fast frequency bands, in **figure 5** indicated by the pink lines, reflect *short range* activity and the response to external stimulation and, finally, the ultra-slow range, which is associated with intrinsic processes (Hramov et al., 2015; Pavlov et al., 2012). One possible interpretation of this oscillation in the ultra-slow range can be given in terms of frequency modulation (Brazhe et al., 2006; Sosnovtseva et al., 2005). The idea is that the intrinsic ultra-slow dynamics modulate the stimulus driven frequency. Similar to the modulation of the heart rate by breathing- the duration of beat-to-beat intervals varies at different breathing frequencies. The existence of rhythms in the bold signal leads to the appearance of *ridges* in the energy surface, associated with the rhythmic contributions (Addison, Watson, & Feng, 2002; Amor et al., 2005; Hramov et al., 2015). The dynamics of rhythmic components hidden in a bold signal is reflected in the time evolution of the spectral ridges. Spectral ridges are local maxima of the energy density spectrum at fixed times $t_0$. (the maxima of the bright areas in **figure 5**). Oscillation of spectral ridges indicates the presence of a given rhythm in the bold signal dynamics and its modulation by other rhythms. In detail, if a region, or its underlying neurons, generates a stereotypic response to periodic stimulation, then its

instantaneous frequency associated with the stimulus rhythm remains constant, resulting in a perfect, continuous and straight, spectral ridge at the stimulus frequency (Hramov et al., 2015). Deviation from the stereotypic response would be reflected as temporal variations in the instantaneous frequency. The greater the fluctuations, the more significant the differences in the BOLD response. These ridges, oriented along the time axis, identify the spectral content of the BOLD signal at any given time moment (Addison et al., 2002; Amor et al., 2005). If the stability measure is high, then the bold response is highly repeatable during the whole recording, and consequently, such an answer is likely to be using a kind of temporal code. Conversely, low stability suggests high variability in the spike patterns, origin of the bold signal, and points to a rate code or the presence of a complex dynamics, for example, involving local and global feedback and fast adaptation.

In the frequency domain, spectral coherence is a well-established standard tool to analyze the linear relationship between two (usually continuous) signals by determining the correlation between their spectra (Baccalá & Sameshima, 2001; Dahlhaus, Eichler, & Sandkühler, 1997; Hramov et al., 2015). A high spectral coherence suggests the presence of a functional association between, e.g., the stimulus and the neural response in the corresponding frequency band (in our case, the presence of a functional coupling between the vmPFC and the Nacc in the high frequency band). Wavelet coherence, in addition, informs about the functional coupling, but it also provides the temporal structure of the coupling. The temporal structure of the coupling is reflected by the black arrows (see In **figure 6**): horizontal arrows indicate a synchronous coherence without temporal delay, deviation from the horizontal position indicate a temporal delay- the greater the degree the longer the temporal delay (Hramov et al., 2015; Pavlov et al., 2012). In **figure 6** a graphic representation of the 5-blocs task structure with white lines indicating the beginning and the end of experimental blocs. During the intervals between task blocs, only a fixation cross was presented.

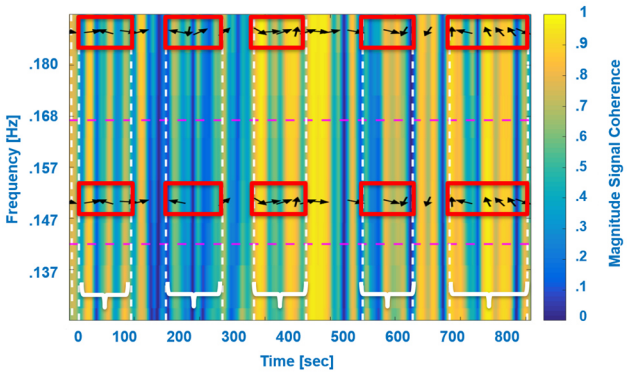


Figure 6 shows spectral coherence between NAcc and vmPFC during processing of the 5-CSRTT. black arrows represent coupling, horizontal position indicate a synchronous coherence without temporal delay, deviation from the horizontal position indicate a temporal delay.

In this analysis, we addressed wavelet parameters of both, task-based and rs-fMRI time courses of the NAcc and vmPFC. The following wavelet parameters were determined: (1) energy density: maximum in the stimulus-induced frequency band was determined (the frequencies between the pink lines, **figure 5**), (2) the frequency value F(t) and (3) stability as defined as the standard deviation of $F$ yields to $St$. On the basis of the modulation hypothesis (i.e. frequencies in the ultra-slow range modulate stimulus-driven frequencies), (4) the modulating frequency (Fmod) as well as (5) its amplitude (MFmod), (6) Ffm the ultra-low peak looking at energy spectrum computed via fourier and (7) Pmf amplitude of the peak at Fmod computed via fourier were determined and statistically analyzed. Finally, spectral coherence was quantified in terms of (8) mean percent duration of sustained coherence relative to scan time, averaged over the stimulus band (meanperc). We expected to find under task processing that lowImp subjects presented a higher stability in the high frequency band in the vmPFC compared to highImp subjects, reflecting the stronger frontal top-down regulation. In addition, we assumed a stronger, more robust modulation of high frequencies by the ultra-slow frequency in lowImp subjects, representing the more effective coupling between the NAcc and the vmPFC in lowImp compared to highImp. In contrast, we expected to find highImp subjects' higher energy in combination with deviation of the modulating frequency reflecting the imbalance between reward-driven NAcc and controlling vmPFC.

# Study 2- Methods

## Participants

We examined 103 male students aged from 19 to 28 years (24.0±2.6 years) (S Neufang et al., 2016). Subjects were recruited at the University of Wuerzburg, Germany. The sample size exceeded the minimal sample size of n=60 for repeated measures analysis of variance (ANOVA) models with within–between interaction as determined by G*Power (http://www.gpower.hhu.de/). All subjects were screened for impulsivity and right-handedness was ascertained using the Edinburgh Handedness Inventory (Oldfield, 1971). The study was approved by the ethics committee of the Faculty of Medicine, University of Würzburg, and was conducted in accordance with the Declaration of Helsinki in its latest version from 2008. Written informed consent was obtained from all subjects.

## Wavelet Transforms and Statistical Analysis

To quantify the stability of the bold response, the following measure can be considered:

$$St = \frac{1}{\sigma_0},$$

where $\sigma_0$ is the standard deviation of the time evolution of the main spectral ridge found in the vicinity of the stimulus frequency. To evaluate $St$ for the bold signal, its energy density is estimated after leaving out all the signal components that are not part of the frequency stimulus band. For a fixed time $t_0$, the energy maximum in the stimulus frequency band was searched. To each value corresponds a frequency value that evaluates with time, $F(t_0)$. The standard deviation of $F$ yields to $St$ quantifying how stable bold responses are. To prove the existence of a modulation we used the double wavelet-technique on the energy maxima of only the stimulus- induced high frequency band (Hramov et al., 2015). Finally, spectral coherence was determined in terms of frequency-specific correlations (Yaesoubi et al., 2015). Group comparisons were performed using two sample t-tests. To correct for multiple comparisons, FDR-correction was applied. In addition to factorial analyses correlations were performed in order to address linear relations between impulsivity and wavelet parameters.

## Study 2- Results

The two most powerful frequency bands in the fMRI signal corresponded to a fast frequency band around .15 Hz and a slow frequency bands around .05. Fluctuation in these frequency bands were related to task processing- as they were only increased under task condition and not at rest (see **figure 7**). However, in the ultra-slow frequency around .01 a common and stable peak was found, which remained in the spectrum in both conditions. *Frequency Modulation.* We found that instantaneous amplitude as well as frequency fluctuated with a frequency of exactly .011 Hz, which means at our ultra-slow frequency. The spectral ridges were continuous and straight, indicating a robust and stable modulation process (see **figure 8**). *Spectral Coherence*. Interestingly, we found, that whereas during task-blocs a coupling was present, during rest phases, the coupling vanished hinting towards a highly efficient processing of the brain- in terms of using resting phases to actual rest (see **figure 6**). Two sample t-tests did not reveal any significant difference between impulsivity groups. Uncorrected for multiple comparisons, however, highImp showed a higher stability in the vmPFC compared to lowImp during task processing, in combination with a higher modulating frequency (stronger deviation from the ultra-slow frequency).

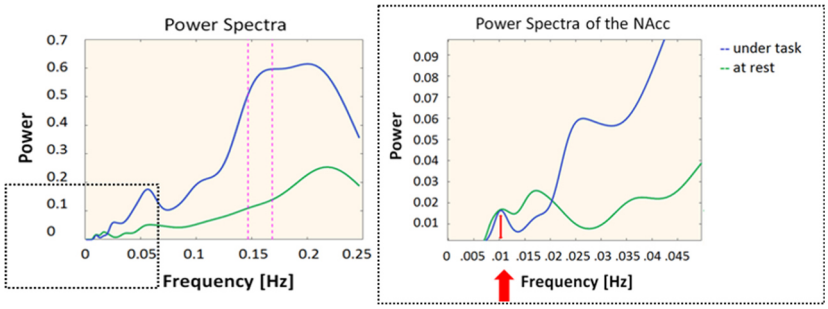


Figure 7 Power spectrum of task- fMRI and rs-fMRI timecourses
The red arrow indicates a common peak at 0.01 Hz. NAcc: nucleus accumbens

In the NAcc, energy at rest was significantly higher in highImp compared to lowImp, accompanied by a longer time coupled at rest (see **table 3** and **figure 9**).

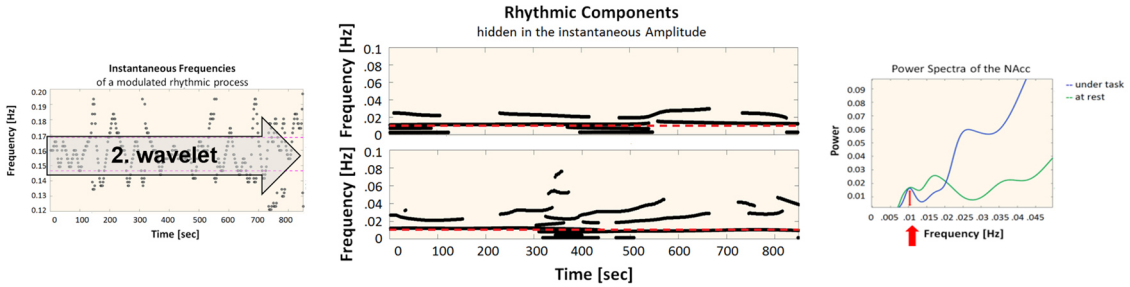


Figure 8 shows the workflow of the determination of frequency modulation

On the dimensional level, the relation between impulsivity and stability in the NAcc under task differed significantly between groups: whereas in lowImp the stability increased with impulsivity, there was no relation in highImp. Likewise, frequency amplitude increased significantly with impulsivity in lowImp whereas there was a trend wise negative relation in highImp subjects.

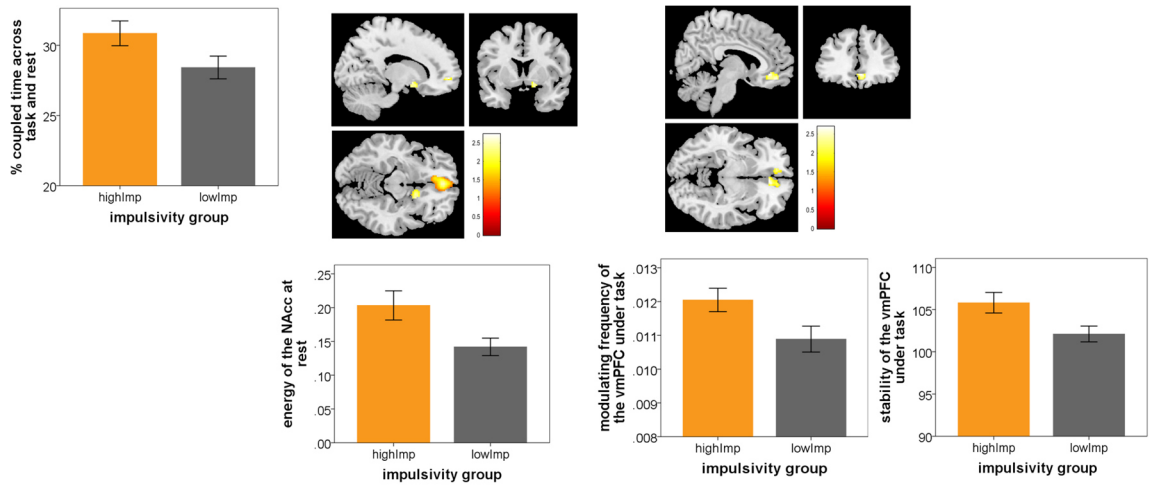


Figure 9 shows differences between highImp and lowImp in wavelet parameters.

## Study 2- Discussion

In this analysis we addressed wavelet parameters with regard to their influence of trait impulsivity. In line with earlier findings analyses revealed, that under task processing lowImp subjects presented a higher stability in the vmPFC compared to highImp subjects, suggesting a stronger impulse control (Nicholas A Donnelly et al., 2014; Voon, 2014; Worbe et al., 2014) and/or a more stable neural network of impulse control (Qiu, 2007; Wu, Zhou,

Xiang, & Liu, 2009; Yang & Xu, 2005). At rest, energy in the NAcc was significantly higher in highImp compared to lowImp (Mechelmans et al., 2017), which might be interpreted in terms of an inefficient processing at rest (Hossein-Zadeh, Ardekani, & Soltanian-Zadeh, 2003; Kang, Pae, & Park, 2017; Schultze-Kraft, Becker, Breakspear, & Ritter, 2011). The latter was supported by the finding, that spectral coherence between the vmPFC and NAcc at rest, was longer in highImp compared to low impulsive subjects, i.e. highImp did not 'uncouple' at rest (Niazy, Xie, Miller, Beckmann, & Smith, 2011; Yaesoubi et al., 2015). A similar phenomenon has been reported in the context of drug craving the way the stronger the craving the longer the coherence between the amygdala and the dorsal cingulate cortex at rest (Lam et al., 2013) interpreted as an ineffective way of brain functioning. Finally, we, indeed, found that stimulus-driven frequency was stronger modulated by the ultra-slow frequency in lowImp subjects compared to highImp, hinting towards a robust coupling within the WI network in lowImp subjects.

Unfortunately to date, publications of wavelet transforms using fMRI time series are predominantly methodological reports and do not address alterations of parameters with regard to either psychological traits and / or psychiatric disorders. However, its potential in the context of the same is discussed in the General Discussion Section / Time-frequency Information of the WI Network.

Table 3 Results from group comparisons on wavelet parameters using two sample t-tests

| | lowImp | highImp | T(2,101), p | lowImp | highImp | T(2,101), p |
|---|---|---|---|---|---|---|
| task-fMRI | | | | | | |
| energy | .18(.12) | .24(.16) | 1.9, .07 | .09(.06) | .10(.07) | 0.4, .71 |
| frequency | .16(.00) | .16(.00) | 0.4, .69 | .16(.00) | .16(.00) | 1.5, .13 |
| stability | 103.6(3.4) | 104.5(3.4) | 1.4, .18 | 102.1(6.2) | 105.8(9.3) | 2.3*, .03 |
| Fmod | .01(.00) | .01(.00) | 0.4, .70 | .01(.00) | .01(.00) | 2.2*, .03 |
| MFmod | .01(.01) | .02(.01) | 1.9, .05 | .02(.02) | .02(.02) | 0.5, .64 |
| Ffm | .16(.01) | .15(.00) | 0.5, .60 | .16(.01) | .16(.01) | 1.0, .32 |
| Pmf | 8.4(7.4) | 11.4(8.4) | 1.9, .06 | 3.6(2.2) | 3.6(2.2) | 0.1, .94 |
| mperc | 31.8(6.5) | 31.4(5.7) | 0.3, .74 | | | |
| rs-fMRI | | | | | | |
| energy | .14(.09) | .20(1.7) | 2.2*, .03 | .11(.08) | .11(.09) | 0.3, .78 |
| frequency | .17(.00) | .16(.00) | 0.1, .89 | .16 (.01) | .16(.00) | 0.8, .43 |
| stability | 103.3(4.7) | 102.7(4.4) | 0.6, .52 | 102.4(3.4) | 102.8(4.4) | 0.5, .60 |
| Fmod | .01(.00) | .01(.00) | 0.7, .51 | .01(.00) | .01(.00) | 0.8, .44 |
| MFmod | .02(.02) | .02(.02) | 1.6, .11 | .03(.03) | .03(.03) | 0.5, .57 |
| Ffm | .16(.01) | .16(.01) | 0.4, .64 | .16(.01) | .16(.01) | 1.4, .15 |
| Pmf | 6.4(5.5) | 8.0(6.9) | 1.3, .20 | 5.2(5.4) | 5.0(5.8) | 0.2, .87 |
| mperc | 28.0(5.4) | 28.5(6.0) | .44, .66 | | | |
| mperc_tot | 28.4(5.4) | 30.9(6.8) | 2.0*, .05 | | | |

Note. Fmod: modulating frequency, MFmod: mean amplitude of modulating frequency, Ffm: ultra-low peak, Pmf: amplitude of the peak at Fmod, mperc: mean duration of coherence, $p_{FDR}$/q*=.003, *: p<.05, uncorrected.

# Study 3- AFA, WI Network

## Study 3- Introduction

Fractal structures possess the property that the whole structure consists of parts, which have the same pattern composition but at different scales and/or in different sizes (Koch, 1904, 1906; B. Mandelbrot, 1967; B. B. Mandelbrot, 1983). Fractals can also be found in dynamic processes; *scale invariance* (P. Ivanov et al., 2009; Nagy et al., 2017; Suckling et al., 2008) means that both, rapidly occurring changes and slowly proceeding dynamics follow the same structure, or better, that measures of the patterns are independent of the sampling rate, used during data acquisition (Riley et al., 2012). For time series, this property is mathematically expressed as follows:

$$S(f) = \frac{C_f}{|f|^{\beta}} \qquad \text{and } \beta = 2H - 1$$

$S(f)$ represents the power spectrum density of the analyzed fluctuations, $f$ the frequency, $C_f$ a constant and 0 < $\beta$ < 2. Furthermore, $\beta$ is related to the $H$. For more details on how to compute $H$ refer to method section fractal analysis as suggested by Riley et al. (Riley et al., 2012).

Fractal patterns have been examined in many research fields including physiology (Sen & McGill, 2018) and neuroscience (Di Ieva et al., 2015; Di Ieva et al., 2014). A specific phenomenon called *pink noise* (also called fractal or 1/f noise, with $\beta = 1$) is one of the key fractal manifestations. Pink noise is a stochastic process, used for the modelling of dynamic systems (Deif, 2012; Deif & ElMaraghy, 2009). Its power spectral density (PSD) is inversely proportional to the sample frequency (A. Eke et al., 2000; A. Eke, Herman, Kocsis, & Kozak, 2002; Keshner, 1982). Because pink or 1/f noise lies between white noise ($1/f^0$, or random noise), and red/Brownian noise ($1/f^2$, power density decreases with increasing frequency), it has been proven to bring stability and adaptability into dynamic processes, thus, crucial properties of well-functioning complex systems (Bak, Tang, & Wiesenfeld, 1987). Pink noise has been documented in behavioral as well as physiological processes, for example in heartbeat dynamics (Plamen Ch Ivanov, Amaral, Goldberger, & Havlin, 1999; P. C. Ivanov et al., 2001), neural network organization (Lewis A. Lipsitz, 2002; L. A. Lipsitz & Goldberger, 1992) and cognitive processes (Ihlen & Vereijken, 2010; Wijnants, Cox, Hasselman, Bosman, & Van Orden, 2012). The manifold appearance of pink noise has led to the speculation, that "there exists some profound law of nature that applies to all nonequilibrium systems and results in such noise" (Sejdić & Lipsitz, 2013). Intuitively, one might assume that pink noise has a detrimental effect to a system's performance and accuracy. However, as pink noise arises from the interaction of multiple systems and operates

over different scales, it has been shown to contribute to system resiliency and structural integrity if individual components were lost or interrupted for example by age or disease (Lewis A. Lipsitz, 2002; L. A. Lipsitz & Goldberger, 1992). A fractal network structure, thus, qualifies a system to cope with stress or disturbances by adjusting specific components and fine tuning its responses (for a review see Sejdić & Lipsitz, 2013).

Pink noise can be found in the fMRI signal (see **figure 10**) (S. Behseta & Chenouri, 2011; Bullmore et al., 2009; Churchill et al., 2016; Ciuciu, Abry, & He, 2014; Ciuciu et al., 2012; Andras Eke et al., 2012; Herman, Sanganahalli, Hyder, & Eke, 2011; Nagy et al., 2017). $H$ valued close to 1 in the fMRI signal has been associated with a higher predictability of time series (Gentili et al., 2017), greater low-frequency power and higher persistence over time (Ball et al., 2011), as well as highly complex and well attuned dynamics in the underlying network (Goldberger et al., 2002; L. A. Lipsitz & Goldberger, 1992). Likewise, it has been shown that deviation from pink noise in relevant parameters, independent of whether the changes occurred in the direction of white or red noise, was associated with neurological as well as psychiatric disorders (e.g. reaction time sequences in ADHD: Gilden & Hancock, 2007; rs-fMRI in Alzheimer's disease: Maxim et al., 2005).

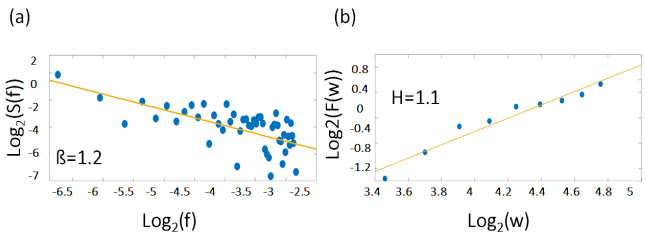


Figure 10 The 1/f noise pattern in a power spectrum (Eq1) of an exemplary time course is shown on logarithmic scales while the scale invariance relation (Eq3) is indicated by the slope $H$. Please note, that the relationship between $\beta$ and $H$ is according to eq2 $\beta = 2H - 1$. For demonstration, the example of a representative individual time course of the right MFG during task has been used.

In addition, fractality seems to be more pronounced in low compared to high frequencies. For example, Fox et al. (2007) reported 1/f noise in the fMRI signal (Fox, Snyder, Vincent, & Raichle, 2007), emphasizing that "spontaneous BOLD follow a 1/f distribution, meaning that there is an increasing power in the low frequencies." (Fox & Raichle, 2007). In addition, Gentili et al., (2017) found brain regions where $H$ as well as metrics of low-frequency oscillations (i.e. amplitude of low-frequency fluctuations, ALFF, fractional amplitude of low-frequency fluctuations, fALFF) had similar effects hinting towards strong relation between both measures (Gentili et al., 2017). In task-fMRI data, fractal noise of inactive voxels differed from those of active ones (Thurner, Windischberger, Moser, Walla, & Barth, 2003). Recent rs-fMRI-studies showed, that $H$ correlated with personality traits (Gentili et al., 2017; Gentili et al., 2015) as well as behavioural task performance (Wink et al., 2008). For example, anxiety (Gentili et al., 2015) and extraversion (Gentili et al., 2017) correlated positively with $H$ in regions

of the default mode network and response time in a attention task with $H$ in the inferior frontal gyrus (Wink et al., 2008) (i.e. the shorter the reaction times, the higher $H$) hinting towards an influence of both personality traits and task performance on the persistence of network dynamics (Wink et al., 2008). Likewise, findings from task-fMRI studies reported that $H$ decreased with task processing (Ciuciu et al., 2012) and cognitive effort (Barnes et al., 2009; Churchill et al., 2016) concluding that "task-related modulation of multifractality appears only significant in functional networks and thus can be considered as the key property disentangling functional networks from artifacts." (Ciuciu et al., 2012). A first study addressing the influence of impulsivity on $H$ revealed that impulsivity correlated negatively with $H$ in the orbito-frontal cortex (i.e. the vmPFC) and NAcc (Hahn et al., 2012) the way that the higher impulsive the subjects the smaller the $H$.

In this study, we examined the fractal nature of a brain network associated with WI using the AFA approach. $H$ was determined for all network regions at rest and while performing the 5-CSRTT. To define, whether a subject is high (highImp) or low impulsive (lowImp), the number of premature responses has been used (e.g. N. A. Donnelly et al., 2014; Feja et al., 2014). Based on the introduced findings we were intrigued to address the existence of pink noise in our network, thus, we expected to find (a) a fractal nature of the impulsivity network and that fractality consists of pink noise, i.e. $H$ values of all network regions were close to 1 (e.g. Fox & Raichle, 2007; Fox et al., 2007). (b) smaller $H$ at task compared to rest (Barnes et al., 2009; Churchill et al., 2016; Ciuciu et al., 2012). (c) significant influence of impulsivity on $H$ predominantly in the PFC and the NAcc (Hahn et al., 2012; Wink et al., 2008). In line with the previous studies (Gilden & Hancock, 2007; Hausdorff, 2007) we expected to find deviation from 1/f noise pronounced in highImp compared to lowImp subjects.

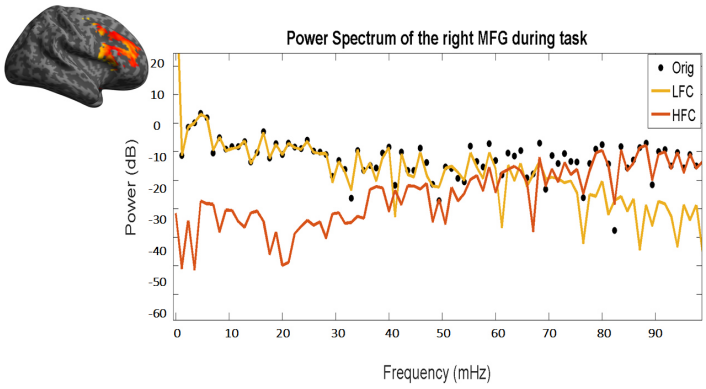


Figure 11 shows the power frequency spectrum of the original time course (black dots), as well as of the resulting low (yellow line) and high frequency (red line) components. Please note the overlap between the black dots (original time course) and the yellow line (LFC) in low frequencies (left part of the x-axis) and between the black dots and the red line (HFC) in high frequencies (right part of the x-axis). The same time course of the right MFG during task of a representative subjects has been used.

# Study 3- Methods

## AFA.

Fractal analysis of time series is based on quantifying the degree of fluctuation around the overall trend of the data over time, to measure the scale invariance quantified by the value of $H$ (see equation below). In this

paper, we split the fMRI signal into two components: the low and the high frequency components (LFC, HFC) (see **figure 11**). LFC is the second order polynomial that is a smooth and global fit of the original time course (see **figure 12**). HFC represents the residuals after subtracting the fitting curve from the original time course. For time series to be fractal, their PSD must be inversely proportional to frequency (see also **figure 13**, legend). After analyzing these two main components, we found, that the residuals were more likely to obscure the results with respect to the scale invariance analysis. HFC, in addition, could not be classified as fractal (see **figure 13**). The low frequency component of the signal on the other hand, held all the information concerning the fractal nature of the original signal. In line with earlier studies and to avoid inaccuracies and the reduction of $H$, we focused in our analyses on those parts of the signal/those regions, which showed power law scaling and fractal scaling was present (e.g. Cannon, Percival, Caccia, Raymond, & Bassingthwaighte, 1997; Herman et al., 2011; Riley et al., 2012): only the LCF was taken into consideration for further analysis via AFA to compute $H$.

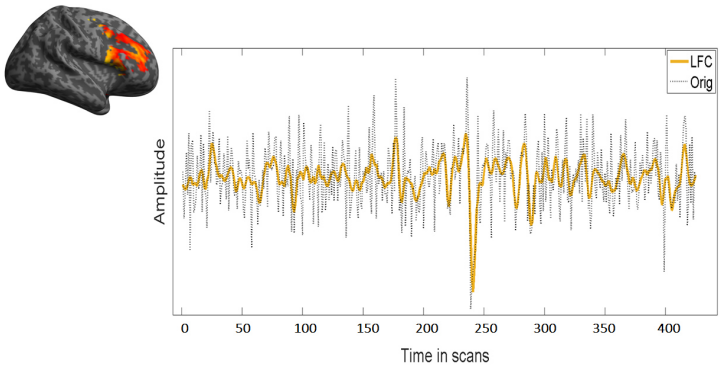


Figure 12 shows the overlap between low frequency course (LFC) and the original time course. LFC fits well the data without overfitting leaving out unnecessary information for the fractal analysis. In this figure, the same time course of the right MFG during task of a representative subjects has been used.

AFA is one of the existing mathematical methods that computes $H$, a factor that reflects in a scale law manner the relationship, that is intrinsic to fractal processes, between the variance of fluctuation computed around, in our case, a second order polynomial trend $v(i)$ fitted to time series within each segment $w$, and its size:

$$F(w) = \left[\frac{1}{N}\sum_{i=1}^{N}\left(u(i) - v(i)\right)^2\right]^{1/2} \sim w^H,\ N\text{: length of the time series}$$

$$w = 2n + 1, n = 5,6 \ldots,13$$

$H$ is determined as the slope of the log-log diffusion plot $log_2\left(F(w)\right)$ as a function of $log_2(w)$ (see **figure 10b**).

## Statistical Analysis

A permutation test was performed to ensure the validity of using the number of premature responses as grouping criteria. The question of the existence of pink noise was verified using a one sample Wilcoxon test with $H$ of all network regions as test variables and 1 as hypothetical median. The following statistical analyses were performed:

(i) To compare fractality at rest and while task processing, non-parametric tests of related samples were defined using the within-subject factor *condition* (task vs. rest), and $H$ as dependent variable. To reveal the impact of the impulsive phenotype on differences between rest and task, the same analyses were performed phenotype-specifically.

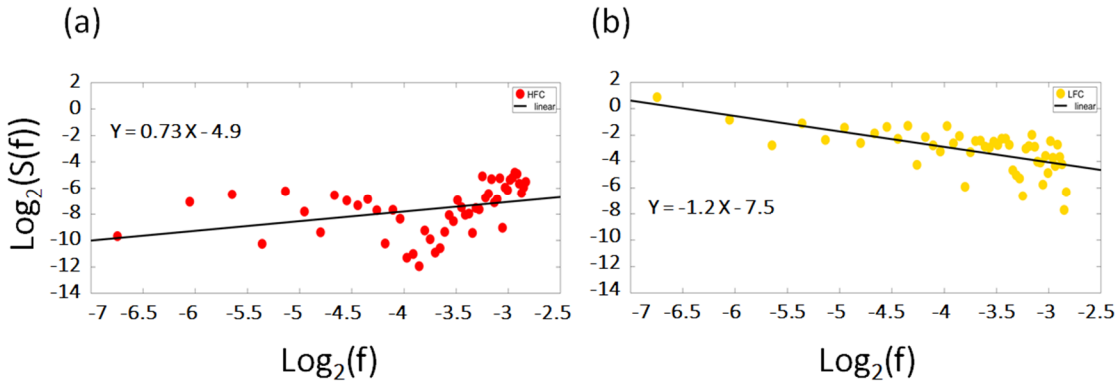


Figure 13 shows the log-log diffusion plots of the power spectrum density (PSD) of the low and high frequency components (LFC, HFC): whereas the HFC (red dots) fails to fulfill the criteria of a fractal structure expressed by Eq1, the PSD of the LFC (yellow dots) is clearly inversely proportional to frequency hinting toward a fractal nature. The data presented is the same time course of the right MFG during task of a representative subjects.

(ii) The influence of impulsivity on network fractality was performed using both, the factorial and the dimensional approach. Impulsive phenotype differences of $H$ were addressed using non-parametric Mann-Whitney-U-Test for 2 independent samples using the between-subject factor *impulsive phenotype* and dependent variables were $H$ scores. In addition, correlations between WI (i.e. the number of premature responses, task accuracy, reward and reaction times) and $H$ scores were performed.

For all statistical analyses a significance threshold of $p<0.05$, corrected for multiple comparisons using the False-Discovery Rate (Benjamini & Hochberg, 1995a), was applied. The number of test as well as q*-scores representing the FDR-corrected significance levels were provided for each analysis in the results section as well as in tables 1 and 2.

## Study 3- Results

Post-Hoc power analyses using G*Power (version 3.1.9.3, http://www.gpower.hhu.de/) revealed a power of .77 and a critical Z=1.6. Performed fMRI analyses revealed that whereas activation bilaterally in the middle frontal gyrus (MFG) (right MFG: x=40, y=.8, 34, T=19.7; left MFG: x=-44, y=6, 28, T=21.7), the ACC (x=6, y=30, 28, T=18.6)

as well as the vmPFC (x=0, y=48, -12, T=6.5) was associated with impulse control, bilaterally the HC (right HC: x=24, y=-28, -6, T=21.9; left HC: x=-22, y=-28, -6, T=17.7), the right NAcc (x=8, y=12, -10, T=14.6), and the left amygdala (x=-22, y=0, -12, T=6.0) were active while reward processing (see **figure 14**). Via AFA we found that (a) at rest across all subjects, $H$ was similar to 1 in the following network regions (rHC: M=0.93±0.13, p=.000; lHC: M=0.96±0.12, p=.000; lMFG: M=1.01±0.12, p=.156; rMFG: M=1.00±0.12, p=.577; ACC: M=1.01±0.12, p=.414; rNAcc: M=1.03±0.10, p=.060; lAMY: M=1.00±0.11, p=.928; vmPFC: M=1.01±0.12, p=.087, corrected for 8 comparisons with q*=.006) proving a stable fractal nature of this network.

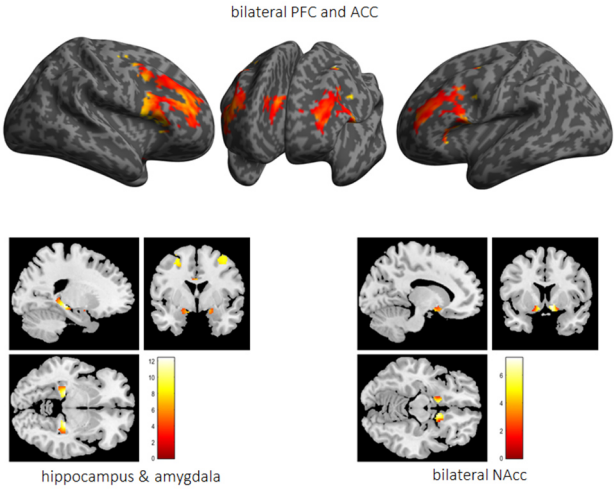


Figure 14 presents the impulsivity network
in terms of significantly activated brain regions across all subjects while performing the 5-choice serial reaction time task. PFC: prefrontal cortex, ACC: anterior cingulate cortex, Nacc: nucleus accumbens

(b) Across all subjects (i.e. independent of the impulsive phenotype), $H$ was significantly higher at rest compred to task in all regions. Group-specific analyses, however, revealed that in highImp subjects, fractality in the right HC did not differ at rest and during task processing (see **table 4**). In lowImp subjects, $H$ was significantly higher at rest compared to task in all regions.

(c) $H$ during task-processing differed between impulsivity phenotypes in terms of reduced $H$ in highImp subjects in the reward-associated NAcc and the impulse control-related ACC (see **table 5**). Furthermore, $H$ of the left HC varied trend-wisely between impulsivity groups across. At rest, there was no significant difference in any region.Correlations revealed a significant correlation between $H$ of the left MFG and the number of premature responses (r=.-.242, p=.013, corrected for 16 comparisons with q*=.012).

Table 4 Comparison of H between task and rest across all subject

| | lowImp | | | highImp | | |
|---|---|---|---|---|---|---|
| | task [M(SD)] | rest [M(SD)] | Z | task [M(SD)] | rest [M(SD)] | Z |
| rHC | 0.88(.11) | 0.94(.13) | 3.4** | 0.88(.11) | 0.92(.12) | n.s. |
| lHC | 0.91(.10) | 0.96(.13) | 2.6** | 0.88(.10) | 0.95(.10) | 2.8** |
| lMFG | 0.94(.11) | 1.02(.11) | 4.1** | 0.90(.12) | 1.00(.12) | 3.5** |
| rMFG | 0.93(.14) | 1.00(.13) | 2.7** | 0.90(.12) | 1.00(.12) | 3.6** |
| ACC | 0.96(.13) | 1.02(.13) | 2.8** | 0.89(.09) | 0.99(.10) | 4.1** |
| rNAcc | 0.93(.13) | 0.98(.12) | 2.3** | 0.87(.13) | 1.00(.12) | 2.9** |
| lAMY | 0.89(.12) | 0.92(.12) | n.s. | 0.86(.11) | 0.95(.14) | 2.7** |
| vmPFC | 0.98(.11) | 1.07(.12) | 4.2*** | 0.97(.11) | 0.91(.12) | 3.3** |

Note. rHC: right hippocampus, lHC: left hippocampus, lMFG: left middle frontal gyrus, rMFG: right middle frontal gyrus, ACC: anterior cingulate cortex, Nacc: nucleus accumbens, lAMY: left amygdala, vmPFC: ventromedial prefrontal gyrus; lowImp: low impulsive subjects, highImp: high impulsive subjects, FDR-corrected was applied for 8 comparisons, corrected significance level were q*(all subjects) =.05, q*(highImp subjects) =.04, q*(highImp subjects) =.04, **: p< q*, n.s.: not sig

# Study 3- Discussion

In this study, we addressed the fractal nature of a neural network associated with WI. We found (a) pink noise in all network regions, proving the existence of a fractal nature within this network (Bak et al., 1987; Lewis A. Lipsitz, 2002; L. A. Lipsitz & Goldberger, 1992; Wijnants et al., 2012). Furthermore, (b) $H$ was significantly higher at rest compared to task. This was the case in all regions and across all subjects. However, in highImp subjects, $H$ was comparable during task-fMRI and at rest in the right HC. (c) Finally, during task processing, fractality in impulse control related left MFG as well as reward associated NAcc and ACC was influenced by impulsivity the way that in highImp subjects $H$ was significantly smaller and, therefore, was a less adequate 1/f noise fit candidate compared to lowImp subjects.

Table 5 H in highImp and lowImp, M(SD)

| | lowImp | highImp | Z |
|---|---|---|---|
| task-fMRI | | | |
| rHC | 0.87(.11) | 0.88(.11) | 0.2 |
| lHC | 0.91(.10) | 0.88(.10) | 1.9 |
| lMFG | 0.94(.11) | 0.90(.11) | 1.7 |
| rMFG | 0.93(14) | 0.90(.11) | 1.1 |
| ACC | 0.96(.13) | 0.89(.09) | 3.0** |
| rNAcc | 0.93(.13) | 0.87(.13) | 2.4** |
| lAMY | 0.89(.11) | 0.86(.11) | 1.4 |
| vmPFC | 0.98(.11) | 0.97(.11) | 0.6 |
| rs-fMRI | | | |
| all regions | n.s. | | |

Note. rHC: right hippocampus, lHC: left hippocampus, lMFG: left middle frontal gyrus, rMFG: right middle frontal gyrus, ACC: anterior cingulate cortex, Nacc: nucleus accumbens, lAMY: left amygdala, vmPFC: ventromedial prefrontal gyrus, $_{low}$: low impulsive subjects, $_{high}$: high impulsive subjects; FDR-corrected was applied for 16 comparisons, corrected significance level was q*=.007, **: p<q*, n.s.: not significant.

## Fractality during task processing and at rest

Higher fractality at rest compared to task processing / cognitive effort is in line with earlier findings (S. Behseta & Chenouri, 2011; Churchill et al., 2016; Ciuciu et al., 2012). In the context of the common knowledge, that neural networks are predominantly active after an external stimulation, e.g. of our senses

or while cognitive processing (Kandel, Schwartz, & Jessel, 2000; Penn & Shatz, 1999), this finding seems counter-intuitive. However, the recent years of research on the brain at rest have accentuated the prominence of endogenously engendered brain responses as an important defining factor in modeling the topology of large-scale neuronal networks (for review see V. D. Calhoun & de Lacy, 2017; Gorges et al., 2017; Liegeois, Laumann, Snyder, Zhou, & Yeo, 2017; Linkenkaer-Hansen, 2002). The terms used most frequently to describe resting-state neural activity, such as "endogenous", "intrinsic" and "spontaneous", indicate that network function is created within the brain itself, and can, thus, be understood as "self-organized" (Linkenkaer-Hansen, 2002). Self-organized criticality, in return, has been described by Bak et al., (1987) as the origin of fractal objects. They demonstrated, that "dynamic systems naturally evolve into self-organized critical structures of states" and suggested, that "this self-organized criticality is the common underlying mechanism" behind those dynamic system (Bak et al., 1987). For an empirical example in the context of sleep dynamics, Lo et al (2013) were able to identify two independent paths for the transition between sleep phases using power-law scaling on nocturnal EEG recordings (Lo, Bartsch, & Ivanov, 2013). Thus, a task-induced stimulation operating as an involvement from the outside system may lead to a reduction of these dynamics, hence of fractality.

In highImp subjects, however, $H$ did not decrease significantly during task in the right HC. A generally small fractality in the hippocampus has been reported by He et al. (2014). They found varying $H$ across different cortical regions with lowest $H$ in the HC, interpreting these findings in terms of regional differences in neurovascular coupling mechanisms (S. Behseta & Chenouri, 2011; He, 2014). Impaired hippocampal $H$ has also been reported between patients with Alzheimer's disease and control subjects (Maxim et al., 2005) with the persistence of $H$ being assumed to reflect neurodegenerative processes. The insignificant change of $H$ during task processing in high impulsive subjects in our study, thus, might reflect a weaker recruitment of the right HC while performing the task and a more superficial learning (e.g. El-Gaby, Shipton, & Paulsen, 2015). In return, this finding can also be interpreted the way, that the right HC is less adaptive in high impulsive subjects, thus constantly following its own dynamics, leading to an impaired motivation- or reward-based learning of the task (Chantiluke et al., 2012; Moreno-Lopez, Soriano-Mas, Delgado-Rico, Rio-Valle, & Verdejo-Garcia, 2012).

## Fractality differs in function of impulsivity

Our analyses revealed, that impulsivity modulated fractality only during task processing and predominantly in the fronto-striatal loop namely the ACC and the NAcc. $H$ in the left MFG, in addition, correlated negatively with

behavioral impulsivity. Morris et al. (2015) showed that functional connectivity in the ACC and the NAcc via the subthalamic nucleus varied in function of the number of premature responses (L. S. Morris et al., 2016) emphasizing the crucial and interacting role of these two structures on the key parameter of WI. Functional connectivity in the left MFG as part of the dorsolateral PFC, in return, reflects the counterpart, i.e. top-down control which decreases with higher reward processing (Mechelmans et al., 2017).

In the NAcc as well as in the ACC, in high impulsive subjects, $H$ was significantly reduced compared to low impulsive subjects. A negative association between impulsivity/reward sensitivity and the ventral striatum has been reported by Hahn et al. (2012) before in the way that the higher impulsive/reward sensitive the subjects were, the smaller the $H$ (Hahn et al., 2012). Reduced $H$ in the NAcc and ACC in high impulsive subjects of our study, thus, reflects an altered reward processing.

In addition, significant correlations between impulsivity and fractality in the frontal cortex have been shown for the orbito-frontal cortex (Hahn et al., 2012) as well as for the lateral PFC (Ball et al., 2011). Similar to these findings, we found a significant (negative) correlation with the number of premature responses and $H$ in the left MFG across all subjects as well as in the vmPFC in the highImp group. The MFG is strongly involved in response inhibition and cognitive control (Bari & Robbins, 2013; Boehler, Appelbaum, Krebs, Hopf, & Woldorff, 2010; Braver, 2012; C. D. Chambers, H. Garavan, & M. A. Bellgrove, 2009), thus, a more random top-down control in highImp subjects reflects impaired control and more impulsive task performance. In contrast to findings by Wink et al., $H$ of network regions associated with waiting impulsivity did not correlate with reaction time (Wink et al., 2008). This, however, might be based on the different anatomical structures: Wink et al. reported a correlation of $H$ and rs-fMRI signals in the right inferior frontal cortex, which was not included in our network.

Taken together, the combination of impaired top-down control and altered reward processing is common and has been described for numerous impulse control disorders such as ADHD (e.g. Scheres & Hamaker, 2010), eating disorders (for review Citrome, 2015), addiction (Weinstein, 2017), bipolar disorder, and depression (Carver, Johnson, & Joormann, 2008).

# General Discussion

In this work, three different methodological approaches have been presented and our results have shown, that they were(if present) in line with findings in the same field and performed with conventional fMRI data analyses. In the last closing chapter, the additional information will be discussed in more detail to summarize the benefit of using fMRi data with new statistical approaches.

## BARS-specific information of neural processing in humans

In study 1, we aimed to prove that BARS applied on human fMRI time courses reflect neural processing as it is the case in the modeling of neural responses of electrophysiological recordings in rodents. We argue that the present findings are in line with earlier findings from EEG and fMRI studies as well as from animal and human studies.

The application of BARS on fMRI data, to date, has mainly been theoretically in terms of BARS acting as "a flexible denoiser for fMRI time courses, where all smooth sources of variation are combined into the function being estimated", and serving as "a front-end to spatial and regional analyses and group comparisons, automatically incorporating variation in response shape and magnitude across the replicated task blocks in the experiment" (DiMatteo et al., 2001). Therefore, this is the first fMRI study empirically applying the BARS approach on fMRI time courses and contrasting it with the standard fMRI data analysis to explore the validity of the approach in cognitive processing, instead of a methodological one. Thus, we relied on the theoretical combination of statistical (fluctuations of λ(t) of the BOLD signal) and neuroscientific findings (amplitude and timing of the BOLD signal reflect gamma and beta power). However, to empirically prove the validity of these assumptions, we directly compare findings from BARS (new approach) with findings from GLM analyses (standard approach) of the same data set as a first dataset specific validation and discuss them in the context of earlier findings in terms of a second external validation. This way we aimed to undermine that BARS is a valid statistical approach to look at characteristics of the BOLD response beyond the usual activation and connectivity patterns.

Nevertheless, it is crucial to gain more experience especially with this approach because BARS address brain activation data in terms of curves, not condition-specific activation patterns. To interpret the findings, a change of perspective is needed. For example, Behseta and Chenouri (2011) compared curves of neuronal data between two populations and their reports predominantly consist of the description of differences between groups in curve shapes (S. Behseta & Chenouri, 2011; Muniz-Terrera et al., 2016). In our study, we also found that differences

were bin-specific, which means they were only significantly different in certain periods of time. For example, gamma power in the left PFC was enhanced in bad performers only in the last quarter of the task. Does this finding reflect a stronger need for concentration in bad performers as compared to good performers at the end of the task based on a higher fatigue in this group? Or is it more likely that this is based on general differences in fluctuations in this region over the course of the whole experiment but significantly only within these bins? To better understand the information provided by BARS from fMRI data, further studies are crucial and needed.

Furthermore, we propose BARS as a potential statistical approach for data analysis across species. In the present human fMRI study, we were not able to directly relate our findings to neurophysiological recordings measuring gamma and beta power, so the transfer of results relied on literature references and had to be considered theoretically. Therefore, a translational study design would be of high interest, including both neurophysiological recordings from rodents and fMRI time courses from humans acquired while performing the same behavioral paradigm (e.g. the 5-CSRTT; animal version: Robbins, 2002; human version: Voon et al., 2014). Species-specific neural data could be analyzed with BARS to extract neural firing / BOLD responses facilitating the direct comparison of findings, and also to improve the interpretation of human results significantly.

Based on the current findings, we conclude that the present results suggest performance variations to be associated with alterations in BOLD amplitude and its temporal dynamics of frontal top-down and bottom-up parietal processing. Based on the relationship between neural signaling and BOLD response, we argue that bad performance is associated with both increased activation and gamma power in the left PFC, along with a reduced brain activation and an increased beta power in the parietal and striatal areas. With regard to the harmonization of translational study protocols, BARS seem to be a promising tool for data analysis.

## Time-frequency Information of the WI Network

Using wavelet transforms as performed in study 2, we were able to split the fMRI signal into several frequencies. This means, the fMRI time courses were not described in terms of temporal fluctuation and amplitude of the entire fMRI signal as presented in study 1 but in temporal fluctuations and amplitudes at different frequencies (Meyer, 2003; Unser & Aldroubi, 1996). We could show, that signals at different frequencies were not random but reflected different aspects of neural network processing, so that we were able to get a deeper insight into how the brain works.

Different frequency bands and the reflected neural processes have been described for animals as well as in humans using single cell recording and EEG recordings (Canolty & Knight, 2010; Harris, Hirase, Leinekugel, Henze, & Buzsáki, 2001; Pfurtscheller & Da Silva, 1999; Teplan, 2002). The idea that not only in EEG and single cell recording but also in fMRI, frequency bands and frequency-specific fluctuations might play a role in the signal interpretation of cognitive processing comes from the theory of *neural network synchronization*. This theory was adapted from the neural binding hypothesis by Singer and Gray (1995), according to which synchronous oscillations in spatially distributed neuronal ensembles bind neurons representing different features of an object (Singer & Gray, 1995). Transferring this idea into connectivity networks, Honey et al. (2007) simulated spontaneous neuronal firing (millisecond timescale) for a network giving rise to spatial and temporal patterns of synchronous oscillations: "The link between fluctuations in transfer entropy and, at a similar time scale, in fMRI timeseries appears to be mediated by the relationship between the synchronization of neuronal dynamics and the mean activity of neuronal populations. Importantly, it suggests that empirical fMRI signals may reflect the time-varying fast synchronization of population dynamics." (Honey, Kötter, Breakspear, & Sporns, 2007). One might argue, that temporal scales might differ between neuronal oscillations and low frequency BOLD fluctuations, thus, synchronization is not confined to oscillations of the same frequency band but occurs across different frequencies as n:m synchrony (Palva, Palva, & Kaila, 2005; Tognoli & Kelso, 2009).

With regard to the role of frequencies in fMRI, low frequency fluctuations have been described between 0.01 and 0.08 Hz (Salvador et al., 2008) or <0.1 Hz (Biswal, Kylen, & Hyde, 1997), and also higher frequency bands (up to 0.16 Hz) have been identified as relevant in resting state network (Niazy et al., 2011). These frequency ranges seemed to be independent of the used functional connectivity measures [e.g. small world architecture (Achard, Salvador, Whitcher, Suckling, & Bullmore, 2006; Supekar, Menon, Rubin, Musen, & Greicius, 2008; Supekar, Musen, & Menon, 2009), wavelet-based networks parameters (Ginestet & Simmons, 2011), resting state networks (Lagioia, Van De Ville, Debbané, Lazeyras, & Eliez, 2010)], however, network-specific. For example Smyser et al. (2010) found highest signal peaks within the sensori-motor cortex at 0.02–0.04 Hz , in contrast to much broader range of 0.01–0.05 Hz in visual networks (Smyser et al., 2010). For attention networks induced by the ANT, bottom-up connections were associated with frequencies within the frequency range <.03 Hz, hinting towards spatial processing and cue-based attentional orienting. In contrast, top-down connectivity was associated with frequencies >0.08 Hz, which might be interpreted as the reflection of an active, intensive cognitive processing

(Akhrif, Bajer, Wohlschläger, Konrad, & Neufang, 2013b; Neufang et al., 2014). In this line, recent theories regarding the interaction between frequencies as suggested in study 2 add a new perspective, even though these theories need more elaborate scientific research.

## The Fractal Nature of the WI Network

In study 3, we addressed the fractal nature of a neural network associated with WI. We found that (a) pink noise in all network regions, proving the existence of a stable fractal nature within this network (Bak et al., 1987; Lewis A. Lipsitz, 2002; L. A. Lipsitz & Goldberger, 1992; Wijnants et al., 2012).

As introduced we learned that a brain network follows a stable fractal patterns when $H$ is close to 1 (e.g. Stadnitski, 2012), is decreased while cognitive activation (Barnes et al., 2009; Churchill et al., 2016; Ciuciu et al., 2012), and is sensitive to normal and abnormal alteration such as disease or age (Lewis A. Lipsitz, 2002; L. A. Lipsitz & Goldberger, 1992; Sejdić & Lipsitz, 2013). In our data, we could find all these aspects and, hence, assumed a fractal nature in the impulsivity network: at rest, $H$ varied around 1 across all subjects; during task processing, $H$ was significantly reduced in all regions and, finally, when comparing $H$ between high and low impulsive subjects, $H$ was reduced in highImp subjects in some of the network regions. The network examined here has been introduced in a comprehensive review article by Dalley et al. (2011) and is based on relevant findings from humans and animal studies on impulsivity and cognitive top-down control (Jeffrey W Dalley et al., 2011). The notion that the suggested network regions were indeed involved in the processes of WI as measured via the 5-CSRTT has been shown in recent studies (dlPFC and ACC: Mechelmans et al., 2017; NAcc and ACC: Laurel S Morris et al., 2016; e.g. NAcc and vmPFC: S Neufang et al., 2016). The characterization of this network as a "healthy and complex system" (Bak et al., 1987), however, has been demonstrated in this study for the first time.

In contrast to earlier studies, in which $H$ was determined on the whole brain level and in a data-driven manner (e.g. Barnes et al., 2009; Churchill et al., 2016; Gentili et al., 2017; Gentili et al., 2015; Suckling et al., 2008; Wink et al., 2008), we chose to focus on an earlier described network. This way, we were able to *a priori* match cognition and neural structures, however, taking the risk of losing information, for example regarding the compensatory recruitment of additional structures. When examining a clinical sample, thus, a combined approach would be indicated. In this study, we chose a monofractal approach. The main reasons were the following: (1) This is a pilot study for a clinical project; thus, data acquisition was strongly determined by the factors (a) field strength (3T) (b) total scanning time (12min / 365 volumes during rs-fMRI; 14min / 420 volumes during task), (c) sample rate

(2000ms) to ensure the feasibility for patients to perform the scanning procedure successfully. In contrast to animal studies, data quality is very poor as all factors play a crucial role in the analysis of fractal patterns in fMRI (Andras Eke et al., 2012). For example, the field strength highly influences measurement sensitivity (A. Eke, Herman, & Hajnal, 2006) and multi-fractal analysis is "known to require a much higher signal definition for an optimal performance" than monofractal (Ciuciu et al., 2012; Andras Eke et al., 2012). Likewise, multi-fractal analyses need longer time series / higher sampling rates than those found for monofractal series (A. Eke et al., 2002; Andras Eke et al., 2012). In a previous step multi-fractality was addressed (using q from -2 to 2) and revealed, that our signals are, with no loss of information, to be approximated as monofractal (**figure 15**). The monofractal approximation, however, has been proven to be a robust assumption and, thus, an adequate tool to address similar signals. And it has one advantage- it is human data.

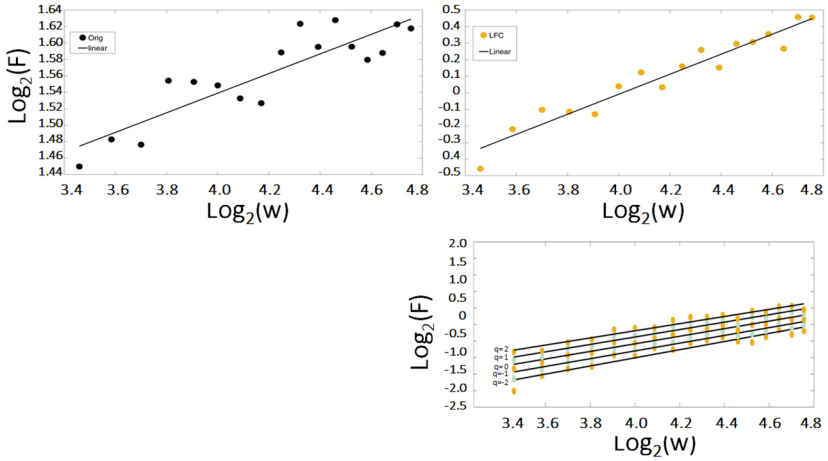


Figure 15 shows: the scaling function f and the corresponding regression line of the entire signal (left upper row) and for its LFC only (right upper row). Please note that data points in the case of the LFC are linearly fitted, whereas this is not the case in the entire signal. The diagram in the lower row shows that the slopes H of the regression lines are q-indepenent (monofractal). For this diagramm, MFDFA has been used (Ihlen, 2012). For demonstration, the example of a representative individual time course has been used.

The use of fractal parameters to examine neural networks regarding to health or disorder has been described in earlier studies (e.g. Dona, Noseworthy, DeMatteo, & Connolly, 2017; El-Gaby et al., 2015; Gorges et al., 2017; Hahn et al., 2012; Lei, Zhao, & Chen, 2013; Lewis A. Lipsitz, 2002; Maxim et al., 2005; Sokunbi et al., 2014), introducing these parameters as exceptionally sensitive towards alterations. In our study, however, we performed analysis in a very homogenous sample of young adult male students. The classification into high and low impulsive subjects, therefore, is relative and does not represent samples with manifest impulse control disorders. The transfer of the present data to a clinical context therefore predominantly relies on the findings of earlier studies and would be of high interest for future studies.

Thus, we would like to emphasize, that the use of fractality and $H$ in particular, has two advantages which makes it a promising biomarker in the early detection of disease: (i) the reference score is a concrete number (i.e. 1) the

difference can be interpreted as a measure of the deviation from this reference, (ii) in principle the assessment of $H$ can be integrated in the (f)MRI clinical routine protocol subject to the availability of sufficiently long fMRI-BOLD sequences. However – consistent with earlier observations with various fractal time series methods (A. Eke et al., 2000)-, as stated by Riley et al. (2012), "AFA requires careful consideration of signal properties, parameter settings, and interpretation of results, and should not be applied blindly to unfamiliar signals." (Riley et al., 2012). In line with earlier studies, our data showed the potential of fractal parameters in the detection of altered brain function in the clinical context. For that reason, it is highly recommended to follow up on the development of methods to making fractal analysis accessible to a wider public and delivering unambiguous results.

## Limitation and Conclusion

In sum, this dissertation provided new insights into the information MRI signals contain. The used methodological approaches are well established mathematical frameworks, however, their application on fMRI, to date, is new. The overall aim was to identify statistical methods apt for the analysis of species-overlapping data. However, in this dissertation only human data was analyzed. As no animal data was available, parameters were analyzed regarding 'conventional' human behavioral phenotypes (i.e. good performer vs. bad performer, highImp vs. lowImp) and discussed predominantly theoretical in the scientific debate of translational studies.

In addition, in this dissertation parameters were determined in networks, associated with 'higher' cognitive processing, i.e. in attention and impulsivity networks. Thus, neural processing is much more inhomogeneous compared to e.g. visual processing. However, relating neural complexity (visual vs. impulsivity) and potential clinical relevance (with a potential neuropsychiatric impact, e.g. in the context of ADHD), the latter was chosen. The point has already been raised before and we would like to generalize it as follows:

Taken together, we would like to emphasize, that the use of parameters as performed in this dissertation enables us to find promising biomarker in the early detection of diseases, even though human data is not as pure as in animal or technical data sets. Therefore, it is highly recommended to follow up on the development of methods to making these analyses applicable to a wider set of data and delivering results for a wider range of relevance for humans.

# References


Achard, S., Salvador, R., Whitcher, B., Suckling, J., & Bullmore, E. (2006). A resilient, low-frequency, small-world human brain functional network with highly connected association cortical hubs. *Journal of Neuroscience, 26*(1), 63-72.

Addison, P., Watson, J., & Feng, T. (2002). Low-oscillation complex wavelets. *Journal of Sound and Vibration, 254*(4), 733-762.

Ahn, S., Zauber, S. E., Worth, R. M., & Rubchinsky, L. L. (2016). Synchronized beta-band oscillations in a model of the globus pallidus-subthalamic nucleus network under external input. *Frontiers in computational neuroscience, 10*, 134.

Akhrif, A., Bajer, C., Wohlschläger, A. M., Konrad, K., & Neufang, S. (2013a). Development-related dynamics in a top-down control network. *Journal of Neuroscience and Neuroengineering, 2*(3), 255-266.

Akhrif, A., Bajer, C., Wohlschläger, A. M., Konrad, K., & Neufang, S. (2013b). Frequency-specific top-down modulation within a fronot-parietal network. *Journal of Neuroscience and Neuroengineering, 2*, 272.

Alexander, G. E., DeLong, M. R., & Strick, P. L. (1986). Parallel organization of functionally segregated circuits linking basal ganglia and cortex. *Annu Rev Neurosci, 9*, 357-381. doi:10.1146/annurev.ne.09.030186.002041

Alho, J., Green, B. M., May, P. J., Sams, M., Tiitinen, H., Rauschecker, J. P., & Jääskeläinen, I. P. (2016). Early-latency categorical speech sound representations in the left inferior frontal gyrus. *Neuroimage, 129*, 214-223.

Amor, F., Rudrauf, D., Navarro, V., N'diaye, K., Garnero, L., Martinerie, J., & Le Van Quyen, M. (2005). Imaging brain synchrony at high spatio-temporal resolution: application to MEG signals during absence seizures. *Signal processing, 85*(11), 2101-2111.

Axmacher, N., Henseler, M. M., Jensen, O., Weinreich, I., Elger, C. E., & Fell, J. (2010). Cross-frequency coupling supports multi-item working memory in the human hippocampus. *Proceedings of the National Academy of Sciences, 107*(7), 3228-3233.

Baccalá, L. A., & Sameshima, K. (2001). Overcoming the limitations of correlation analysis for many simultaneously processed neural structures *Progress in brain research* (Vol. 130, pp. 33-47): Elsevier.

Bak, P., Tang, C., & Wiesenfeld, K. (1987). Self-organized criticality: An explanation of the 1/f noise. *Phys Rev Lett, 59*(4), 381-384. doi:10.1103/PhysRevLett.59.381

Ball, G., Stokes, P. R., Rhodes, R. A., Bose, S. K., Rezek, I., Wink, A. M., . . . Turkheimer, F. E. (2011). Executive functions and prefrontal cortex: a matter of persistence? *Front Syst Neurosci, 5*, 3. doi:10.3389/fnsys.2011.00003

Balleine, B. W., & O'doherty, J. P. (2010). Human and rodent homologies in action control: corticostriatal determinants of goal-directed and habitual action. *Neuropsychopharmacology, 35*(1), 48.

Bari, A., & Robbins, T. W. (2013). Inhibition and impulsivity: behavioral and neural basis of response control. *Prog Neurobiol, 108*, 44-79. doi:10.1016/j.pneurobio.2013.06.005

Barnes, A., Bullmore, E. T., & Suckling, J. (2009). Endogenous human brain dynamics recover slowly following cognitive effort. *PLoS One, 4*(8), e6626. doi:10.1371/journal.pone.0006626

Behseta, S., & Chenouri, S. (2011). Comparison of two populations of curves with an application in neuronal data analysis. *Stat Med, 30*(12), 1441-1454. doi:10.1002/sim.4192

Behseta, S., & Kass, R. E. (2005). Testing equality of two functions using BARS. *Statistics in medicine, 24*(22), 3523-3534.

Benjamini, Y., & Hochberg, Y. (1995a). Controlling the False Discovery Rate: A Practical and Powerful Approach to Multiple Testing. *Journal of the Royal Statistical Society. Series B (Methodological), 57*(1), 289-300.

Benjamini, Y., & Hochberg, Y. (1995b). Controlling the false discovery rate: a practical and powerful approach to multiple testing. *Journal of the Royal statistical society: series B (Methodological), 57*(1), 289-300.

Benson, S., Tiplady, B., & Scholey, A. (2019). Attentional and working memory performance following alcohol and energy drink: A randomised, double-blind, placebo-controlled, factorial design laboratory study. *PLoS One, 14*(1), e0209239. doi:10.1371/journal.pone.0209239

Biswal, B. B., Kylen, J. V., & Hyde, J. S. (1997). Simultaneous assessment of flow and BOLD signals in resting-state functional connectivity maps. *NMR in Biomedicine, 10*(4-5), 165-170.

Boehler, C. N., Appelbaum, L. G., Krebs, R. M., Hopf, J. M., & Woldorff, M. G. (2010). Pinning down response inhibition in the brain--conjunction analyses of the Stop-signal task. *Neuroimage, 52*(4), 1621-1632. doi:10.1016/j.neuroimage.2010.04.276

Braver, T. S. (2012). The variable nature of cognitive control: a dual mechanisms framework. *Trends Cogn Sci, 16*(2), 106-113. doi:10.1016/j.tics.2011.12.010

Brazhe, N., Brazhe, A., Pavlov, A., Erokhova, L., Yusipovich, A., Maksimov, G., . . . Sosnovtseva, O. (2006). Unraveling cell processes: interference imaging interwoven with data analysis. *Journal of Biological Physics, 32*(3-4), 191-208.

Brett, M., Anton, J.-L., Valabregue, R., & Poline, J.-B. (2002). *Region of interest analysis using an SPM toolbox.* Paper presented at the 8th international conference on functional mapping of the human brain.

Breukelaar, I. A., Antees, C., Grieve, S. M., Foster, S. L., Gomes, L., Williams, L. M., & Korgaonkar, M. S. (2017). Cognitive control network anatomy correlates with neurocognitive behavior: A longitudinal study. *Human brain mapping, 38*(2), 631-643.

Brown, P., Williams, D., Aziz, T., Mazzone, P., Oliviero, A., Insola, A., . . . Di Lazzaro, V. (2002). Pallidal activity recorded in patients with implanted electrodes predictively correlates with eventual performance in a timing task. *Neuroscience letters, 330*(2), 188-192.

Brunet, N., Vinck, M., Bosman, C. A., Singer, W., & Fries, P. (2014). Gamma or no gamma, that is the question. *Trends Cogn Sci, 18*(10), 507-509. doi:10.1016/j.tics.2014.08.006

Bubenzer-Busch, S., Herpertz-Dahlmann, B., Kuzmanovic, B., Gaber, T., Helmbold, K., Ullisch, M. G., . . . Zepf, F. (2016). Neural correlates of reactive aggression in children with attention-deficit/hyperactivity disorder and comorbid disruptive behaviour disorders. *Acta Psychiatrica Scandinavica, 133*(4), 310-323.

Buckner, R. L., & Koutstaal, W. (1998). Functional neuroimaging studies of encoding, priming, and explicit memory retrieval. *Proceedings of the National Academy of Sciences, 95*(3), 891-898.

Bullmore, E., Barnes, A., Bassett, D. S., Fornito, A., Kitzbichler, M., Meunier, D., & Suckling, J. (2009). Generic aspects of complexity in brain imaging data and other biological systems. *Neuroimage, 47*(3), 1125.

Bullmore, E., Long, C., Suckling, J., Fadili, J., Calvert, G., Zelaya, F., . . . Brammer, M. (2001). Colored noise and computational inference in neurophysiological (fMRI) time series analysis: resampling methods in time and wavelet domains. *Human brain mapping, 12*(2), 61-78.

Burnett Heyes, S., Adam, R. J., Urner, M., van der Leer, L., Bahrami, B., Bays, P. M., & Husain, M. (2012). Impulsivity and Rapid Decision-Making for Reward. *Frontiers in psychology, 3*, 153. doi:10.3389/fpsyg.2012.00153

Buzsáki, G., & Wang, X.-J. (2012). Mechanisms of gamma oscillations. *Annual review of neuroscience, 35*, 203-225.

Calhoun, V. D., Adali, T., Stevens, M., Kiehl, K., & Pekar, J. J. (2005). Semi-blind ICA of fMRI: a method for utilizing hypothesis-derived time courses in a spatial ICA analysis. *Neuroimage, 25*(2), 527-538.

Calhoun, V. D., & de Lacy, N. (2017). Ten Key Observations on the Analysis of Resting-state Functional MR Imaging Data Using Independent Component Analysis. *Neuroimaging Clin N Am, 27*(4), 561-579. doi:10.1016/j.nic.2017.06.012

Cannon, M. J., Percival, D. B., Caccia, D. C., Raymond, G. M., & Bassingthwaighte, J. B. (1997). Evaluating scaled windowed variance methods for estimating the Hurst coefficient of time series. *Physica A, 241*(3-4), 606.

Canolty, R. T., & Knight, R. T. (2010). The functional role of cross-frequency coupling. *Trends in cognitive sciences, 14*(11), 506-515.

Carver, C. S., Johnson, S. L., & Joormann, J. (2008). Serotonergic function, two-mode models of self-regulation, and vulnerability to depression: what depression has in common with impulsive aggression. *Psychol Bull, 134*(6), 912-943. doi:10.1037/a0013740

Cathebras, P., Mosnier, C., Levy, M., Bouchou, K., & Rousset, H. (1994). [Screening for depression in patients with medical hospitalization. Comparison of two self-evaluation scales and clinical assessment with a structured questionnaire]. *Encephale, 20*(3), 311-317.

Chambers, C. D., Garavan, H., & Bellgrove, M. A. (2009). Insights into the neural basis of response inhibition from cognitive and clinical neuroscience. *Neuroscience & biobehavioral reviews, 33*(5), 631-646.

Chambers, C. D., Garavan, H., & Bellgrove, M. A. (2009). Insights into the neural basis of response inhibition from cognitive and clinical neuroscience. *Neurosci Biobehav Rev, 33*(5), 631-646. doi:10.1016/j.neubiorev.2008.08.016

Chantiluke, K., Halari, R., Simic, M., Pariante, C. M., Papadopoulos, A., Giampietro, V., & Rubia, K. (2012). Fronto-striato-cerebellar dysregulation in adolescents with depression during motivated attention. *Biol Psychiatry, 71*(1), 59-67. doi:10.1016/j.biopsych.2011.09.005

Churchill, N. W., Spring, R., Grady, C., Cimprich, B., Askren, M. K., Reuter-Lorenz, P. A., . . . Berman, M. G. (2016). The suppression of scale-free fMRI brain dynamics across three different sources of effort: aging, task novelty and task difficulty. *Sci Rep, 6*, 30895. doi:10.1038/srep30895

Citrome, L. (2015). A primer on binge eating disorder diagnosis and management. *CNS Spectr, 20 Suppl 1*, 44-50; quiz 51. doi:10.1017/s1092852915000772

Ciuciu, P., Abry, P., & He, B. J. (2014). Interplay between functional connectivity and scale-free dynamics in intrinsic fMRI networks. *Neuroimage, 95*, 248-263. doi:10.1016/j.neuroimage.2014.03.047

Ciuciu, P., Varoquaux, G., Abry, P., Sadaghiani, S., & Kleinschmidt, A. (2012). Scale-Free and Multifractal Time Dynamics of fMRI Signals during Rest and Task. *Front Physiol, 3*, 186. doi:10.3389/fphys.2012.00186

Corbetta, M., & Shulman, G. L. (2002). Control of goal-directed and stimulus-driven attention in the brain. *Nature reviews neuroscience, 3*(3), 201.

Dahlhaus, R., Eichler, M., & Sandkühler, J. (1997). Identification of synaptic connections in neural ensembles by graphical models. *Journal of neuroscience methods, 77*(1), 93-107.

Dalley, J. W., Everitt, B. J., & Robbins, T. W. (2011). Impulsivity, compulsivity, and top-down cognitive control. *Neuron, 69*(4), 680-694. doi:10.1016/j.neuron.2011.01.020

Dalley, J. W., Everitt, B. J., & Robbins, T. W. (2011). Impulsivity, compulsivity, and top-down cognitive control. *Neuron, 69*(4), 680-694.

Davis, F. C., Knodt, A. R., Sporns, O., Lahey, B. B., Zald, D. H., Brigidi, B. D., & Hariri, A. R. (2013). Impulsivity and the modular organization of resting-state neural networks. *Cereb Cortex, 23*(6), 1444-1452. doi:10.1093/cercor/bhs126

Deif, A. M. (2012). Dynamic analysis of a lean cell under uncertainty. *International Journal of Production Research, 50*(4), 1127-1139.

Deif, A. M., & ElMaraghy, H. A. (2009). Modelling and analysis of dynamic capacity complexity in multi-stage production. *Production Planning & Control, 20*(8), 737-749.

Deserno, L., Wilbertz, T., Reiter, A., Horstmann, A., Neumann, J., Villringer, A., . . . Schlagenhauf, F. (2015). Lateral prefrontal model-based signatures are reduced in healthy individuals with high trait impulsivity. *Transl Psychiatry, 5*, e659. doi:10.1038/tp.2015.139

Di Ieva, A., Esteban, F. J., Grizzi, F., Klonowski, W., & Martin-Landrove, M. (2015). Fractals in the neurosciences, Part II: clinical applications and future perspectives. *Neuroscientist, 21*(1), 30-43. doi:10.1177/1073858413513928

Di Ieva, A., Grizzi, F., Jelinek, H., Pellionisz, A. J., & Losa, G. A. (2014). Fractals in the Neurosciences, Part I: General Principles and Basic Neurosciences. *Neuroscientist, 20*(4), 403-417. doi:10.1177/1073858413513927

DiMatteo, I., Genovese, C. R., & Kass, R. E. (2001). Bayesian curve-fitting with free-knot splines. *Biometrika, 88*(4), 1055-1071.

Dona, O., Noseworthy, M. D., DeMatteo, C., & Connolly, J. F. (2017). Fractal Analysis of Brain Blood Oxygenation Level Dependent (BOLD) Signals from Children with Mild Traumatic Brain Injury (mTBI). *PLoS One, 12*(1), e0169647. doi:10.1371/journal.pone.0169647

Donnelly, N. A., Holtzman, T., Rich, P. D., Nevado-Holgado, A. J., Fernando, A. B., Van Dijck, G., . . . Paulsen, O. (2014). Oscillatory activity in the medial prefrontal cortex and nucleus accumbens correlates with impulsivity and reward outcome. *PloS one, 9*(10), e111300.

Donnelly, N. A., Holtzman, T., Rich, P. D., Nevado-Holgado, A. J., Fernando, A. B., Van Dijck, G., . . . Dalley, J. W. (2014). Oscillatory activity in the medial prefrontal cortex and nucleus accumbens correlates with impulsivity and reward outcome. *PLoS One, 9*(10), e111300. doi:10.1371/journal.pone.0111300

Dosenbach, N. U., Fair, D. A., Cohen, A. L., Schlaggar, B. L., & Petersen, S. E. (2008). A dual-networks architecture of top-down control. *Trends Cogn Sci, 12*(3), 99-105. doi:10.1016/j.tics.2008.01.001

Durston, S., Davidson, M. C., Tottenham, N., Galvan, A., Spicer, J., Fossella, J. A., & Casey, B. (2006). A shift from diffuse to focal cortical activity with development. *Developmental science, 9*(1), 1-8.

Eke, A., Herman, P., Bassingthwaighte, J. B., Raymond, G. M., Percival, D. B., Cannon, M., . . . Ikrenyi, C. (2000). Physiological time series: distinguishing fractal noises from motions. *Pflugers Arch, 439*(4), 403-415.

Eke, A., Herman, P., & Hajnal, M. (2006). Fractal and noisy CBV dynamics in humans: influence of age and gender. *J Cereb Blood Flow Metab, 26*(7), 891-898. doi:10.1038/sj.jcbfm.9600243

Eke, A., Herman, P., Kocsis, L., & Kozak, L. R. (2002). Fractal characterization of complexity in temporal physiological signals. *Physiol Meas, 23*(1), R1-38.

Eke, A., Herman, P., Sanganahalli, B. G., Hyder, F., Mukli, P., & Nagy, Z. (2012). Pitfalls in Fractal Time Series Analysis: fMRI BOLD as an Exemplary Case. *Front Physiol, 3*.

El-Gaby, M., Shipton, O. A., & Paulsen, O. (2015). Synaptic Plasticity and Memory: New Insights from Hippocampal Left-Right Asymmetries. *Neuroscientist, 21*(5), 490-502. doi:10.1177/1073858414550658

Fan, J., McCandliss, B. D., Fossella, J., Flombaum, J. I., & Posner, M. I. (2005). The activation of attentional networks. *Neuroimage, 26*(2), 471-479. doi:10.1016/j.neuroimage.2005.02.004

Feja, M., Hayn, L., & Koch, M. (2014). Nucleus accumbens core and shell inactivation differentially affects impulsive behaviours in rats. *Prog Neuropsychopharmacol Biol Psychiatry, 54*, 31-42. doi:10.1016/j.pnpbp.2014.04.012

Fell, J., Klaver, P., Lehnertz, K., Grunwald, T., Schaller, C., Elger, C. E., & Fernández, G. (2001). Human memory formation is accompanied by rhinal–hippocampal coupling and decoupling. *Nature neuroscience, 4*(12), 1259.

Fox, M. D., & Raichle, M. E. (2007). Spontaneous fluctuations in brain activity observed with functional magnetic resonance imaging. *Nat Rev Neurosci, 8*(9), 700-711.

Fox, M. D., Snyder, A. Z., Vincent, J. L., & Raichle, M. E. (2007). Intrinsic Fluctuations within Cortical Systems Account for Intertrial Variability in Human Behavior. *Neuron, 56*(1), 171-184. doi:https://doi.org/10.1016/j.neuron.2007.08.023

Fries, P., Scheeringa, R., & Oostenveld, R. (2008). Finding gamma. *Neuron, 58*(3), 303-305.

Friston, K. J., Holmes, A. P., Worsley, K. J., Poline, J. P., Frith, C. D., & Frackowiak, R. S. (1994). Statistical parametric maps in functional imaging: a general linear approach. *Human brain mapping, 2*(4), 189-210.

Gao, Y., Wang, Q., Ding, Y., Wang, C., Li, H., Wu, X., . . . Li, L. (2017). Selective Attention Enhances Beta-Band Cortical Oscillation to Speech under "Cocktail-Party" Listening Conditions. *Front Hum Neurosci, 11*, 34. doi:10.3389/fnhum.2017.00034

Geiger, M. J., Domschke, K., Homola, G. A., Schulz, S. M., Nowak, J., Akhrif, A., . . . Neufang, S. (2016). ADORA2A genotype modulates interoceptive and exteroceptive processing in a fronto-insular network. *Eur Neuropsychopharmacol, 26*(8), 1274-1285. doi:10.1016/j.euroneuro.2016.05.007

Gentili, C., Cristea, I. A., Ricciardi, E., Vanello, N., Popita, C., David, D., & Pietrini, P. (2017). Not in one metric: Neuroticism modulates different resting state metrics within distinctive brain regions. *Behav Brain Res, 327*, 34-43. doi:10.1016/j.bbr.2017.03.031

Gentili, C., Vanello, N., Cristea, I., David, D., Ricciardi, E., & Pietrini, P. (2015). Proneness to social anxiety modulates neural complexity in the absence of exposure: A resting state fMRI study using Hurst exponent. *Psychiatry Res, 232*(2), 135-144. doi:10.1016/j.pscychresns.2015.03.005

Gilden, D. L., & Hancock, H. (2007). Response variability in attention-deficit disorders. *Psychol Sci, 18*(9), 796-802. doi:10.1111/j.1467-9280.2007.01982.x

Ginestet, C. E., & Simmons, A. (2011). Statistical parametric network analysis of functional connectivity dynamics during a working memory task. *Neuroimage, 55*(2), 688-704.

Goldberger, A. L., Amaral, L. A., Hausdorff, J. M., Ivanov, P., Peng, C. K., & Stanley, H. E. (2002). Fractal dynamics in physiology: alterations with disease and aging. *Proc Natl Acad Sci U S A, 99 Suppl 1*, 2466-2472. doi:10.1073/pnas.012579499

Gorges, M., Roselli, F., Muller, H. P., Ludolph, A. C., Rasche, V., & Kassubek, J. (2017). Functional Connectivity Mapping in the Animal Model: Principles and Applications of Resting-State fMRI. *Front Neurol, 8*, 200. doi:10.3389/fneur.2017.00200

Goya-Maldonado, R., Walther, S., Simon, J., Stippich, C., Weisbrod, M., & Kaiser, S. (2010). Motor impulsivity and the ventrolateral prefrontal cortex. *Psychiatry Res, 183*(1), 89-91. doi:10.1016/j.pscychresns.2010.04.006

Hahn, T., Dresler, T., Ehlis, A. C., Pyka, M., Dieler, A. C., Saathoff, C., . . . Fallgatter, A. J. (2012). Randomness of resting-state brain oscillations encodes Gray's personality trait. *Neuroimage, 59*(2), 1842-1845. doi:10.1016/j.neuroimage.2011.08.042

Harris, K. D., Hirase, H., Leinekugel, X., Henze, D. A., & Buzsáki, G. (2001). Temporal interaction between single spikes and complex spike bursts in hippocampal pyramidal cells. *Neuron, 32*(1), 141-149.

Hausdorff, J. M. (2007). Gait dynamics, fractals and falls: finding meaning in the stride-to-stride fluctuations of human walking. *Hum Mov Sci, 26*(4), 555-589. doi:10.1016/j.humov.2007.05.003

He, B. J. (2014). Scale-free brain activity: past, present, and future. *Trends Cogn Sci, 18*(9), 480-487. doi:10.1016/j.tics.2014.04.003

Herman, P., Sanganahalli, B. G., Hyder, F., & Eke, A. (2011). Fractal analysis of spontaneous fluctuations of the BOLD signal in rat brain. *Neuroimage, 58*(4), 1060-1069. doi:10.1016/j.neuroimage.2011.06.082

Hinshaw, S. P. (2017). Attention Deficit Hyperactivity Disorder (ADHD): Controversy, Developmental Mechanisms, and Multiple Levels of Analysis. *Annu Rev Clin Psychol*. doi:10.1146/annurev-clinpsy-050817-084917

Honey, C. J., Kötter, R., Breakspear, M., & Sporns, O. (2007). Network structure of cerebral cortex shapes functional connectivity on multiple time scales. *Proceedings of the National Academy of Sciences, 104*(24), 10240-10245.

Hossein-Zadeh, G. A., Ardekani, B. A., & Soltanian-Zadeh, H. (2003). Activation detection in fMRI using a maximum energy ratio statistic obtained by adaptive spatial filtering. *IEEE Trans Med Imaging, 22*(7), 795-805. doi:10.1109/tmi.2003.815074

Hramov, A. E., Koronovskii, A. A., Makarov, V. A., Pavlov, A. N., & Sitnikova, E. (2015). *Wavelets in neuroscience*: Springer.

Ihlen, E. A. F., & Vereijken, B. (2010). Interaction-dominant dynamics in human cognition: Beyond 1/fα fluctuation. *Journal of Experimental Psychology: General, 139*(3), 436-463.

Ivanov, P., Ma, Q. D., Bartsch, R. P., Hausdorff, J. M., Nunes Amaral, L. A., Schulte-Frohlinde, V., . . . Yoneyama, M. (2009). Levels of complexity in scale-invariant neural signals. *Phys Rev E Stat Nonlin Soft Matter Phys, 79*(4 Pt 1), 041920. doi:10.1103/PhysRevE.79.041920

Ivanov, P. C., Amaral, L. A. N., Goldberger, A. L., & Havlin, S. (1999). Multifractality in human heartbeat dynamics. *Nature, 399*(6735), 461.

Ivanov, P. C., Nunes Amaral, L. A., Goldberger, A. L., Havlin, S., Rosenblum, M. G., Stanley, H. E., & Struzik, Z. R. (2001). From 1/f noise to multifractal cascades in heartbeat dynamics. *Chaos, 11*(3), 641-652. doi:10.1063/1.1395631

Principles of Neuroscience, (2000).

Kang, J., Pae, C., & Park, H. J. (2017). Energy landscape analysis of the subcortical brain network unravels system properties beneath resting state dynamics. *Neuroimage, 149*, 153-164. doi:10.1016/j.neuroimage.2017.01.075

Kass, R. E., Ventura, V., & Brown, E. N. (2005). Statistical issues in the analysis of neuronal data. *Journal of neurophysiology, 94*(1), 8-25.

Kass, R. E., Ventura, V., & Cai, C. (2003). Statistical smoothing of neuronal data. *Network-Computation in Neural Systems, 14*(1), 5-16.

Kaufman, C. G., Ventura, V., & Kass, R. E. (2005). Spline-based non-parametric regression for periodic functions and its application to directional tuning of neurons. *Statistics in medicine, 24*(14), 2255-2265.

Kaufman, D. A., Bowers, D., Okun, M. S., Van Patten, R., & Perlstein, W. M. (2016). Apathy, Novelty Processing, and the P3 Potential in Parkinson's Disease. *Front Neurol, 7*, 95. doi:10.3389/fneur.2016.00095

Keshner, M. (1982). 1/f noise. *Proceeding of the IEEE, 70*(3), 212-218.

Koch, H. v. (1904). Sur une courbe continue sans tangente, obtenue par une construction géométrique élémentaire. *Astron. och Fys., 1*, 681-702.

Koch, H. v. (1906). Une méthode géométrique élémentaire pour l'étude de certaines questions de la théorie des courbes planes. *Acta Math, 30*, 145-174.

Lagioia, A., Van De Ville, D., Debbané, M., Lazeyras, F., & Eliez, S. (2010). Adolescent resting state networks and their associations with schizotypal trait expression. *Frontiers in systems neuroscience, 4*, 35.

Lam, S. C., Wang, Z., Li, Y., Franklin, T., O'Brien, C., Magland, J., & Childress, A. R. (2013). Wavelet-transformed temporal cerebral blood flow signals during attempted inhibition of cue-induced cocaine craving distinguish prognostic phenotypes. *Drug Alcohol Depend, 128*(1-2), 140-147. doi:10.1016/j.drugalcdep.2012.08.018

Lei, X., Zhao, Z., & Chen, H. (2013). Extraversion is encoded by scale-free dynamics of default mode network. *Neuroimage, 74*, 52-57. doi:10.1016/j.neuroimage.2013.02.020

Li, N., Ma, N., Liu, Y., He, X. S., Sun, D. L., Fu, X. M., . . . Zhang, D. R. (2013). Resting-state functional connectivity predicts impulsivity in economic decision-making. *J Neurosci, 33*(11), 4886-4895. doi:10.1523/jneurosci.1342-12.2013

Li, X., Gandour, J., Talavage, T., Wong, D., Dzemidzic, M., Lowe, M., & Tong, Y. (2003). Selective attention to lexical tones recruits left dorsal frontoparietal network. *Neuroreport, 14*(17), 2263-2266.

Liegeois, R., Laumann, T. O., Snyder, A. Z., Zhou, J., & Yeo, B. T. T. (2017). Interpreting temporal fluctuations in resting-state functional connectivity MRI. *Neuroimage*. doi:10.1016/j.neuroimage.2017.09.012

Linkenkaer-Hansen, K. (2002). *self organized criticality and stochastic resonance in the human brain* Dept of Engineering Physics and Mathematics, Helsinki University of Technology, Finland.

Linnet, J. (2014). Neurobiological underpinnings of reward anticipation and outcome evaluation in gambling disorder. *Frontiers in behavioral neuroscience, 8*, 100.

Lipsitz, L. A. (2002). Dynamics of StabilityThe Physiologic Basis of Functional Health and Frailty. *The Journals of Gerontology: Series A, 57*(3), B115-B125. doi:10.1093/gerona/57.3.B115

Lipsitz, L. A., & Goldberger, A. L. (1992). Loss of complexity and aging: Potential applications of fractals and chaos theory to senescence. *JAMA, 267*(13), 1806-1809. doi:10.1001/jama.1992.03480130122036

Lo, C. C., Bartsch, R. P., & Ivanov, P. C. (2013). Asymmetry and Basic Pathways in Sleep-Stage Transitions. *Europhys Lett, 102*(1), 10008. doi:10.1209/0295-5075/102/10008

Logothetis, N. K., Pauls, J., Augath, M., Trinath, T., & Oeltermann, A. (2001). Neurophysiological investigation of the basis of the fMRI signal. *Nature, 412*(6843), 150.

Magri, C., Schridde, U., Murayama, Y., Panzeri, S., & Logothetis, N. K. (2012). The amplitude and timing of the BOLD signal reflects the relationship between local field potential power at different frequencies. *Journal of Neuroscience, 32*(4), 1395-1407.

Mandelbrot, B. (1967). How Long Is the Coast of Britain? Statistical Self-Similarity and Fractional Dimension. *Science, 156*(3775), 636-638. doi:10.1126/science.156.3775.636

Mandelbrot, B. B. (1983). *The Fractal Geometry of Nature*: W. H. Freeman.

Maxim, V., Sendur, L., Fadili, J., Suckling, J., Gould, R., Howard, R., & Bullmore, E. (2005). Fractional Gaussian noise, functional MRI and Alzheimer's disease. *Neuroimage, 25*(1), 141-158. doi:10.1016/j.neuroimage.2004.10.044

Mechelmans, D. J., Strelchuk, D., Donamayor-Alonso, N., Banca, P., Robbins, T. W., Baek, K., & Voon, V. (2017). Reward sensitivity and waiting impulsivity: shift towards reward valuation away from action control. *Int J Neuropsychopharmacol*. doi:10.1093/ijnp/pyx072

Melloni, L., Molina, C., Pena, M., Torres, D., Singer, W., & Rodriguez, E. (2007). Synchronization of neural activity across cortical areas correlates with conscious perception. *J Neurosci, 27*(11), 2858-2865. doi:10.1523/jneurosci.4623-06.2007

Meyer, F. G. (2003). Wavelet-based estimation of a semiparametric generalized linear model of fMRI time-series. *IEEE transactions on medical imaging, 22*(3), 315-322.

Monti, M. M. (2011). Statistical Analysis of fMRI Time-Series: A Critical Review of the GLM Approach. *Frontiers in human neuroscience, 5*, 28-28. doi:10.3389/fnhum.2011.00028

Moreno-Lopez, L., Soriano-Mas, C., Delgado-Rico, E., Rio-Valle, J. S., & Verdejo-Garcia, A. (2012). Brain structural correlates of reward sensitivity and impulsivity in adolescents with normal and excess weight. *PLoS One, 7*(11), e49185. doi:10.1371/journal.pone.0049185

Morris, L. S., Kundu, P., Baek, K., Irvine, M. A., Mechelmans, D. J., Wood, J., . . . Voon, V. (2016). Jumping the Gun: Mapping Neural Correlates of Waiting Impulsivity and Relevance Across Alcohol Misuse. *Biol Psychiatry, 79*(6), 499-507. doi:10.1016/j.biopsych.2015.06.009

Morris, L. S., Kundu, P., Baek, K., Irvine, M. A., Mechelmans, D. J., Wood, J., . . . Voon, V. (2016). Jumping the gun: mapping neural correlates of waiting impulsivity and relevance across alcohol misuse. *Biological psychiatry, 79*(6), 499-507.

Muniz-Terrera, G., Bakra, E., Hardy, R., Matthews, F. E., Lunn, D., & group, F. c. (2016). Modelling life course blood pressure trajectories using Bayesian adaptive splines. *Statistical methods in medical research, 25*(6), 2767-2780.

Muralidharan, A., Jensen, A., Connolly, A., Hendrix, C., Johnson, M. D., Baker, K., & Vitek, J. L. (2016). Physiological changes in the pallidum in a progressive model of Parkinson's disease: Are oscillations enough? *Experimental neurology, 279*, 187-196.

Nagy, Z., Mukli, P., Herman, P., & Eke, A. (2017). Decomposing Multifractal Crossovers. *Front Physiol, 8*, 533. doi:10.3389/fphys.2017.00533

Neufang, S., Akhrif, A., Herrmann, C., Drepper, C., Homola, G., Nowak, J., . . . Romanos, M. (2016). Serotonergic modulation of ‘waiting impulsivity’is mediated by the impulsivity phenotype in humans. *Translational psychiatry, 6*(11), e940.

Neufang, S., Akhrif, A., Herrmann, C. G., Drepper, C., Homola, G. A., Nowak, J., . . . Romanos, M. (2016). Serotonergic modulation of 'waiting impulsivity' is mediated by the impulsivity phenotype in humans. *Transl Psychiatry, 6*(11), e940. doi:10.1038/tp.2016.210

Neufang, S., Akhrif, A., Riedl, V., Forstl, H., Kurz, A., Zimmer, C., . . . Wohlschlager, A. M. (2011). Disconnection of frontal and parietal areas contributes to impaired attention in very early Alzheimer's disease. *J Alzheimers Dis, 25*(2), 309-321. doi:10.3233/jad-2011-102154

Neufang, S., Akhrif, A., Riedl, V., Forstl, H., Kurz, A., Zimmer, C., . . . Wohlschlager, A. M. (2014). Predicting effective connectivity from resting-state networks in healthy elderly and patients with prodromal Alzheimer's disease. *Hum Brain Mapp, 35*(3), 954-963. doi:10.1002/hbm.22226

Neufang, S., Geiger, M. J., Homola, G. A., Mahr, M., Akhrif, A., Nowak, J., . . . Domschke, K. (2015). Modulation of prefrontal functioning in attention systems by NPSR1 gene variation. *Neuroimage, 114*, 199-206. doi:10.1016/j.neuroimage.2015.03.064

Neuper, C., Scherer, R., Wriessnegger, S., & Pfurtscheller, G. (2009). Motor imagery and action observation: modulation of sensorimotor brain rhythms during mental control of a brain-computer interface. *Clin Neurophysiol, 120*(2), 239-247. doi:10.1016/j.clinph.2008.11.015

Niazy, R. K., Xie, J., Miller, K., Beckmann, C. F., & Smith, S. M. (2011). Spectral characteristics of resting state networks *Progress in brain research* (Vol. 193, pp. 259-276): Elsevier.

Nord, C. L., Kim, S. G., Callesen, M. B., Kvamme, T. L., Jensen, M., Pedersen, M. U., . . . Voon, V. (2019). The myeloarchitecture of impulsivity: premature responding in youth is associated with decreased myelination of ventral putamen. *Neuropsychopharmacology*. doi:10.1038/s41386-019-0343-6

Oldfield, R. C. (1971). The assessment and analysis of handedness: the Edinburgh inventory. *Neuropsychologia, 9*(1), 97-113.

Palva, J. M., Palva, S., & Kaila, K. (2005). Phase synchrony among neuronal oscillations in the human cortex. *Journal of Neuroscience, 25*(15), 3962-3972.

Pavlov, A. N., Hramov, A. E., Koronovskii, A. A., Sitnikova, E. Y., Makarov, V. A., & Ovchinnikov, A. A. (2012). Wavelet analysis in neurodynamics. *Physics-Uspekhi, 55*(9), 845.

Peelen, M. V., Heslenfeld, D. J., & Theeuwes, J. (2004). Endogenous and exogenous attention shifts are mediated by the same large-scale neural network. *Neuroimage, 22*(2), 822-830.

Penn, A. A., & Shatz, C. J. (1999). Brain waves and brain wiring: the role of endogenous and sensory-driven neural activity in development. *Pediatr Res, 45*(4 Pt 1), 447-458. doi:10.1203/00006450-199904010-00001

Percival, D. B., & Walden, A. T. (2006). *Wavelet methods for time series analysis* (Vol. 4): Cambridge university press.

Pfurtscheller, G., & Da Silva, F. L. (1999). Event-related EEG/MEG synchronization and desynchronization: basic principles. *Clinical neurophysiology, 110*(11), 1842-1857.

Posner, M. I., & Petersen, S. E. (1990). The attention system of the human brain. *Annu Rev Neurosci, 13*, 25-42. doi:10.1146/annurev.ne.13.030190.000325

Priestley, M. B. (1981). *Spectral analysis and time series* (Vol. 1): Academic press London.

Qiu, J. (2007). Exponential stability of impulsive neural networks with time-varying delays and reaction–diffusion terms. *Neurocomputing, 70*(4-6), 1102-1108.

Ramezan, R., Marriott, P., & Chenouri, S. (2014). Multiscale analysis of neural spike trains. *Stat Med, 33*(2), 238-256. doi:10.1002/sim.5923

Reynolds, J. R., Donaldson, D. I., Wagner, A. D., & Braver, T. S. (2004). Item-and task-level processes in the left inferior prefrontal cortex: positive and negative correlates of encoding. *Neuroimage, 21*(4), 1472-1483.

Riley, M. A., Bonnette, S., Kuznetsov, N., Wallot, S., & Gao, J. (2012). A tutorial introduction to adaptive fractal analysis. *Front Physiol, 3*, 371. doi:10.3389/fphys.2012.00371

Robbins, T. (2002). The 5-choice serial reaction time task: behavioural pharmacology and functional neurochemistry. *Psychopharmacology, 163*(3-4), 362-380.

Roh, S. C., Park, E. J., Shim, M., & Lee, S. H. (2016). EEG beta and low gamma power correlates with inattention in patients with major depressive disorder. *J Affect Disord, 204*, 124-130. doi:10.1016/j.jad.2016.06.033

Rossi, A. F., Pessoa, L., Desimone, R., & Ungerleider, L. G. (2009). The prefrontal cortex and the executive control of attention. *Experimental brain research, 192*(3), 489.

Sala, M., Caverzasi, E., Lazzaretti, M., Morandotti, N., De Vidovich, G., Marraffini, E., . . . Brambilla, P. (2011). Dorsolateral prefrontal cortex and hippocampus sustain impulsivity and aggressiveness in borderline personality disorder. *J Affect Disord, 131*(1-3), 417-421. doi:10.1016/j.jad.2010.11.036

Salvador, R., Martinez, A., Pomarol-Clotet, E., Gomar, J., Vila, F., Sarró, S., . . . Bullmore, E. (2008). A simple view of the brain through a frequency-specific functional connectivity measure. *Neuroimage, 39*(1), 279-289.

Schechtman, E., Noblejas, M. I., Mizrahi, A. D., Dauber, O., & Bergman, H. (2016). Pallidal spiking activity reflects learning dynamics and predicts performance. *Proceedings of the National Academy of Sciences, 113*(41), E6281-E6289.

Scheres, A., & Hamaker, E. L. (2010). What we can and cannot conclude about the relationship between steep temporal reward discounting and hyperactivity-impulsivity symptoms in attention-deficit/hyperactivity disorder. *Biol Psychiatry, 68*(4), e17-18. doi:10.1016/j.biopsych.2010.05.021

Schultz, W. (2006). Behavioral theories and the neurophysiology of reward. *Annu. Rev. Psychol., 57*, 87-115.

Schultze-Kraft, M., Becker, R., Breakspear, M., & Ritter, P. (2011). Exploiting the potential of three dimensional spatial wavelet analysis to explore nesting of temporal oscillations and spatial variance in simultaneous EEG-fMRI data. *Prog Biophys Mol Biol, 105*(1-2), 67-79. doi:10.1016/j.pbiomolbio.2010.11.003

Sebastian, A., Jacob, G., Lieb, K., & Tuscher, O. (2013). Impulsivity in borderline personality disorder: a matter of disturbed impulse control or a facet of emotional dysregulation? *Curr Psychiatry Rep, 15*(2), 339.

Sejdić, E., & Lipsitz, L. A. (2013). Necessity of noise in physiology and medicine. *Computer Methods and Programs in Biomedicine, 111*(2), 459-470. doi:https://doi.org/10.1016/j.cmpb.2013.03.014

Sen, J., & McGill, D. (2018). Fractal analysis of heart rate variability as a predictor of mortality: A systematic review and meta-analysis. *Chaos, 28*(7), 072101. doi:10.1063/1.5038818

Shimazaki, H., & Shinomoto, S. (2007). A method for selecting the bin size of a time histogram. *Neural computation, 19*(6), 1503-1527.

Shomstein, S., Kravitz, D. J., & Behrmann, M. (2012). Attentional control: temporal relationships within the fronto-parietal network. *Neuropsychologia, 50*(6), 1202-1210.

Singer, W., & Gray, C. M. (1995). Visual feature integration and the temporal correlation hypothesis. *Annual review of neuroscience, 18*(1), 555-586.

Smyser, C. D., Inder, T. E., Shimony, J. S., Hill, J. E., Degnan, A. J., Snyder, A. Z., & Neil, J. J. (2010). Longitudinal analysis of neural network development in preterm infants. *Cerebral cortex, 20*(12), 2852-2862.

Sokunbi, M. O., Gradin, V. B., Waiter, G. D., Cameron, G. G., Ahearn, T. S., Murray, A. D., . . . Staff, R. T. (2014). Nonlinear complexity analysis of brain FMRI signals in schizophrenia. *PLoS One, 9*(5), e95146. doi:10.1371/journal.pone.0095146

Sosnovtseva, O., Pavlov, A., Brazhe, N., Brazhe, A., Erokhova, L., Maksimov, G., & Mosekilde, E. (2005). Interference microscopy under double-wavelet analysis: a new approach to studying cell dynamics. *Physical review letters, 94*(21), 218103.

Stadnitski, T. (2012). Measuring Fractality. In Holde, J.G., R. M.A., G. J., & T. K. (Eds.), *Fractal Analyses: Statistical and Methodological Innovations and best practices.* (pp. 22.34). Lausanne, CH: Frontiers in Physiology.

Stephan, K. E., Kasper, L., Harrison, L. M., Daunizeau, J., den Ouden, H. E., Breakspear, M., & Friston, K. J. (2008). Nonlinear dynamic causal models for fMRI. *Neuroimage, 42*(2), 649-662.

Stephan, K. E., Penny, W. D., Moran, R. J., den Ouden, H. E., Daunizeau, J., & Friston, K. J. (2010). Ten simple rules for dynamic causal modeling. *Neuroimage, 49*(4), 3099-3109.

Suckling, J., Wink, A. M., Bernard, F. A., Barnes, A., & Bullmore, E. (2008). Endogenous multifractal brain dynamics are modulated by age, cholinergic blockade and cognitive performance. *J Neurosci Methods, 174*(2), 292-300. doi:10.1016/j.jneumeth.2008.06.037

Supekar, K., Menon, V., Rubin, D., Musen, M., & Greicius, M. D. (2008). Network analysis of intrinsic functional brain connectivity in Alzheimer's disease. *PLoS computational biology, 4*(6), e1000100.

Supekar, K., Musen, M., & Menon, V. (2009). Development of large-scale functional brain networks in children. *PLoS biology, 7*(7), e1000157.

Szczepanski, S. M., Crone, N. E., Kuperman, R. A., Auguste, K. I., Parvizi, J., & Knight, R. T. (2014). Dynamic changes in phase-amplitude coupling facilitate spatial attention control in fronto-parietal cortex. *PLoS biology, 12*(8), e1001936.

Taubman, H., Vaadia, E., Paz, R., & Chechik, G. (2013). A Bayesian approach for characterizing direction tuning curves in the supplementary motor area of behaving monkeys. *J Neurophysiol, 109*(11), 2842-2851. doi:10.1152/jn.00449.2012

Teplan, M. (2002). Fundamentals of EEG measurement. *Measurement science review, 2*(2), 1-11.

Thurner, S., Windischberger, C., Moser, E., Walla, P., & Barth, M. (2003). Scaling laws and persistence in human brain activity. *Physica A: Statistical Mechanics and its Applications, 326*(3), 511-521. doi:https://doi.org/10.1016/S0378-4371(03)00279-6

Tognoli, E., & Kelso, J. S. (2009). Brain coordination dynamics: true and false faces of phase synchrony and metastability. *Progress in neurobiology, 87*(1), 31-40.

Unser, M., & Aldroubi, A. (1996). A review of wavelets in biomedical applications. *Proceedings of the IEEE, 84*(4), 626-638.

Vink, M., Kahn, R. S., Raemaekers, M., van den Heuvel, M., Boersma, M., & Ramsey, N. F. (2005). Function of striatum beyond inhibition and execution of motor responses. *Human brain mapping, 25*(3), 336-344.

Voon, V. (2014). Models of impulsivity with a focus on waiting impulsivity: translational potential for neuropsychiatric disorders. *Current addiction reports, 1*(4), 281-288.

Voon, V., Irvine, M. A., Derbyshire, K., Worbe, Y., Lange, I., Abbott, S., . . . Harrison, N. A. (2014). Measuring "waiting" impulsivity in substance addictions and binge eating disorder in a novel analogue of rodent serial reaction time task. *Biological psychiatry, 75*(2), 148-155.

Vossel, S., Thiel, C. M., & Fink, G. R. (2006). Cue validity modulates the neural correlates of covert endogenous orienting of attention in parietal and frontal cortex. *Neuroimage, 32*(3), 1257-1264.

Wallstrom, G., Liebner, J., & Kass, R. E. (2008). An implementation of Bayesian adaptive regression splines (BARS) in C with S and R wrappers. *Journal of Statistical Software, 26*(1), 1.

Weigl, M., Mecklinger, A., & Rosburg, T. (2016). Transcranial direct current stimulation over the left dorsolateral prefrontal cortex modulates auditory mismatch negativity. *Clinical Neurophysiology, 127*(5), 2263-2272.

Weinstein, A. M. (2017). An Update Overview on Brain Imaging Studies of Internet Gaming Disorder. *Front Psychiatry, 8*, 185. doi:10.3389/fpsyt.2017.00185

Wijnants, M. L., Cox, R. F., Hasselman, F., Bosman, A. M., & Van Orden, G. (2012). Does sample rate introduce an artifact in spectral analysis of continuous processes? *Front Physiol, 3*, 495. doi:10.3389/fphys.2012.00495

Wink, A. M., Bullmore, E., Barnes, A., Bernard, F., & Suckling, J. (2008). Monofractal and multifractal dynamics of low frequency endogenous brain oscillations in functional MRI. *Hum Brain Mapp, 29*(7), 791-801. doi:10.1002/hbm.20593

Worbe, Y., Savulich, G., Voon, V., Fernandez-Egea, E., & Robbins, T. W. (2014). Serotonin depletion induces 'waiting impulsivity'on the human four-choice serial reaction time task: cross-species translational significance. *Neuropsychopharmacology, 39*(6), 1519.

Wu, Q., Zhou, J., Xiang, L., & Liu, Z. (2009). Impulsive control and synchronization of chaotic Hindmarsh–Rose models for neuronal activity. *Chaos, Solitons & Fractals, 41*(5), 2706-2715.

Yaesoubi, M., Allen, E. A., Miller, R. L., & Calhoun, V. D. (2015). Dynamic coherence analysis of resting fMRI data to jointly capture state-based phase, frequency, and time-domain information. *Neuroimage, 120*, 133-142. doi:10.1016/j.neuroimage.2015.07.002

Yang, Z., & Xu, D. (2005). Stability analysis of delay neural networks with impulsive effects. *IEEE Transactions on Circuits and Systems II: Express Briefs, 52*(8), 517-521.

# List of Abbreviations

| | |
|---|---|
| 5-CSRTT | 5 choice serial reaction time task |
| ACC | Anterior Cingulate Cortex |
| ADHD | attention deficit hyperactivity disorder |
| AFA | adaptive fractal analysis |
| ALFF | amplitude of low-frequency fluctuations |
| AMY | amygdala |
| ANT | Attentional Network Task |
| BARS | Bayesian Adaptive regression splines |
| BOLD | Blood-Oxygen-Level-Dependent |
| dlPFC | dorsolateral Pre-Frontal Cortex |
| EEG | electro-encephalogram |
| fALFF | fractional amplitude of low-frequency fluctuations |
| FDR | False-Discovery Rate |
| fMRI | functional Magnetic Resonance Imaging |
| GLM | General Linear Model |
| $H$ | Hurst Exponent |
| HC | hippocampus |
| HFC | high frequency components |
| highImp | high impulsive subjects |
| LFC | low frequency components |
| LFP | local field potentials |
| lowImp | low impulsive subjects |
| lPFC | left prefrontal cortes |
| lSPL: | left superior parietal lobule |
| MFG | Middle Frontal Gyrus |
| NAcc | nucleus accumbens |
| PETH | Peri Event Time Histogram |
| PSD | power spectrum density |
| PSTH | peristimulus-time histograms |
| ROI | Region of Interest |
| PFC | prefrontal cortex |
| rs-fMRI | resting-state fMRI |
| rPFC | right prefrontal cortes |
| rSPL | right superior parietal lobule |
| vmPFC | ventromedial Pre-Frontal Cortex |
| WI | waiting impulsivity |

# Appendix

## Experimental Paradigms

### Study 1- ANT

The used paradigm was the ANT as described in Fan et al. 2005. The ANT requires the participants to determine whether the central arrow out of 5 horizontally arranged arrows pointing left or right. Each trial consisted of five events. First, there was a 400 ms fixation period, followed by a 150 ms warning cue. There was either a non-spatially informative double cue, a spatial cue, or alternatively, no cue was presented. After a cue-target interval of 400 ms, a target was presented for 1050 ms, consisting of the target arrow and 4 context flankers (Fan et al., 2005) (see figure 16).

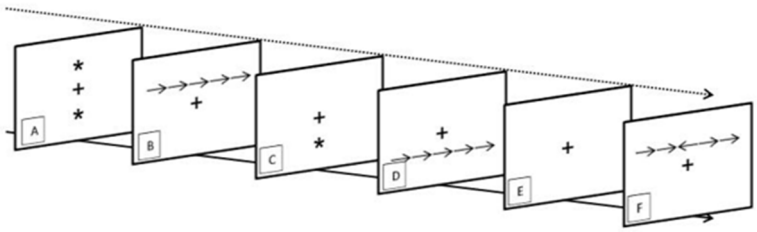


Figure 16 shows an exemplary trial of the ANT.

In order to ensure a variation between stimulus onset and image acquisition, null events were randomly presented in the course of the task. Null events did not represent an experimental condition and thus were not included into the statistical model. Out of 256 trials, there were 64 target events preceded by a double cue, 64 events preceded by a spatially informative cue, 64 events without a cue and 64 null events. In 50% of the experimental trials, targets were congruent (96 trials) and another 50% for incongruent. Trials were presented in a randomized order across all subjects. Total trial duration for null events was 2000 ms, target events were 3000 ms long. Overall, the completion of the task took 14 minutes.

### Studies 2 and 3- 5-CSRTT

The used paradigm was an adapted version of the four-choice serial reaction time task by Voon et al. (Voon et al., 2014) The task consisted of one baseline run outside the scanner and five experimental runs within the scanner. In the task, subjects were instructed to detect a brief visual target after a waiting period to earn a monetary reward. An experimental trial included the following phases/experimental conditions starting with the 'cue' presentation, with the cue representing the start signal and initiating the waiting period (cue-target interval). In contrast to the behavioral task, where subjects had the space bar to keep pushed along the waiting interval, the

start signal in the functional magnetic resonance imaging version was only a visual cue without a following motoric action, due to the minimization of motor artifacts. The second condition was the 'target' onset, the presentation of a green circle in one of the choices and was followed by the subject's response. The trial ended with the reward feedback ('reward' condition): according to the subject's performance, a reward/punishment was administered, showing the amount of recently earned/lost money in combination with the overall amount of earned money. The subjects were instructed to press the corresponding button as fast and as correct as possible (**Figure 17**).

A scanning session included the following steps: outside the scanner, all subjects underwent two training sessions of 10 trials each and a baseline run of 20 trials. To do so, the subjects were seated in front of a computer monitor with a keyboard in front of them (in contrast to touch pad version). In the scanner, subjects lay with response devices in their lap, (Response Grip by Nordic Neuro Lab http://www.nordicneurolab.com/). The baseline run outside the scanner had a duration of 2.5 min, the part within the scanner a total duration of 14 min. Over the course of five runs, WI was manipulated by the following: (a) Implementing a monetary reward: (i) a 1 Euro gain when subjects answered extraordinarily fast and correct, (ii) a 10 Cent win when the subjects reacted in their average velocity and correct and (iii) the loss of 1 Euro when subjects reacted too slow. Incorrect responses did not have consequences.

The criteria for the decision of extraordinarily fast/average/ too slow was determined individually in the first baseline run outside the scanner. In this baseline runs, no reward was implemented, and it served the determination of the individual RT in correct responses. The mean $RT_{M\pm SD}$ was defined as follows: the RT= $RT_{M\pm SD}$→+10 Cent, $RT_{M\pm SD}$.→+1 Euro and RT=$_{M\pm SD}$→−1 Euro. (b) Manipulating the target's presentation duration from 64 ms in the first three experimental runs to 32 ms in the latter runs. (c) Varying of the cue-target interval: whereas in the first two runs the cue-target interval was fix (2000 ms), the duration varied in the last three runs between 2000 and 6500 ms.

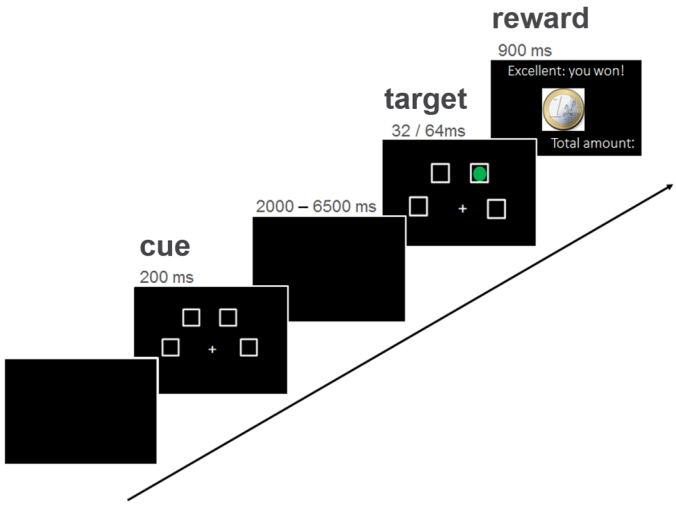


Figure 17 represents one exemplary experimental trial.

(d) Including distractor targets in the last experimental runs in terms of targets with blue and/or yellow circles preceding the actual target.

# fMRI-Data Acquisition

## Study 1

fMRI data was acquired on a 3 Tesla TRIO scanner (Siemens, Erlangen, Germany). Whole-brain T2*-weighted BOLD images were recorded with a gradient echo isotropic 3x3x3mm3 EPI sequence (repetition time TR=2000 ms, echo time TE=30 ms, 36 slices, 3 mm slice thickness, field of view FoV=192 mm, flip angle=90°, 420 volumes). In addition, anatomical images were obtained from each subject using a T1weighted MPRAGE (Magnetization Prepared Rapid Gradient Echo) with the sequence parameters TR=2.3 s, TE=2.95 ms, 176 slices, 1 mm slice thickness, FoV=270 mm, flip angle=9°).

## Studies 2 and 3

The fMRI scanner was a 3 Tesla TIM Trio Scanner (Siemens, Erlangen, Germany). Functional MRI included a T2∗-weighted gradient echo-planar imaging sequence with the following sequence parameters: repetition time (TR) = 2000ms, echo time (TE) = 30ms, 36 slices, 3mm thickness, field of view (FoV) = 192mm, flip angle = 90◦, number of volumes in task-fMRI = 425, number of volumes in rs-fMRI = 350).

# fMRI-Data Preprocessing

## Study 1

fMRI data was pre-processed and analyzed with SPM12 (Wellcome Trust Centre for Neuroimaging London, UK). During preprocessing, all functional images were realigned to the first functional volume for movement correction, unwarped as a correction of field inhomogeneities, spatially normalized into a standard stereotactic space (Montreal Neurological Institute, MNI), resampled to isotropic 2 * 2 * 2 mm3 voxel and spatially smoothed with a Gaussian kernel of 8 mm full width at half maximum (FWHM). Preprocessing did not include high-pass filtering or global mean correction.

The resulting images entered in both analyses, GLM and BARS, in different formats; whereas whole-brain images (sw*.nii) entered GLM-based analyses, region-specific time courses were extracted from pre-processed images (for selection of regions see 3.2.7).

## Studies 2 and 3

Data preprocessing was performed using the Statistical Parametric Mapping Software Package (SPM12). Preprocessing followed the standard routine including temporal and spatial alignment, i.e., slice time correction and realignment and unwarp, spatial normalization [standard space: Montreal Neurological Institute (MNI) space] including a resampling of the data to an isotropic voxel size of 2 × 2 × 2 mm3, spatial smoothing with a Gaussian kernel of 8mm full width at half maximum (FWHM), and linear trend removal [using the matlab routine detrend (y)] (Bai et al., 2008; Zhang et al., 2008; Fox et al., 2009; Qiu et al., 2011). Pre-processing did not include high-pass filtering or global mean correction.

# fMRI time course extraction

## Study 1

For the extraction of fMRI time course, (i) the underlying data is important (in our case the pre-processed data) as well as (ii) the exact localization of the region (i.e. the coordinates of the individual global activation maximum on single subject level).

Regions of Interest (ROI) were areas which have been associated with attention processing in earlier studies (see introduction), namely the prefrontal, parietal and striatal regions. For the identification of global activation

maxima for each subject, the contrast Main Effect of the Attention Network Task was defined on a single subject level and the local maxima of each ROI were identified.

Time course extraction was performed on the pre-processed data. Coordinates were then used as the centre of 10mm spheres using MarsBar (Brett, Anton, Valabregue, & Poline, 2002). Thus, five ROIs (cf. Table 1) were built as the basis of time course extraction for each subject. Following the routine suggested by Brett et al. (2002) (see MarsBar manual, http://marsbar.sourceforge.net/ marsbar.pdf), time courses of raw fMRI data were extracted (i.e. smoothed files resulting from the preprocessing procedure) (Brett et al., 2002).

### Studies 2 and 3

Regions of Interest (ROI) were defined based on the significantly activated brain regions while performing the waiting impulsivity task. In detail, for the identification of global activation maxima, the contrasts target > baseline and reward > baseline were defined on a single subject level and analyzed on group level using a one sample t-test. The local maxima of each significantly activated regions were identified and coordinates were then used as the center of a 10mm spheric ROI using MarsBar [24]. ROIs were built and used for the extraction of the time course for each subject. Time course extraction was performed using the routine as suggested by Brett et al. (2002) (see MarsBar manual, http://marsbar.sourceforge.net/ marsbar.pdf) from preprocessed fMRI data (i.e., smoothed files resulting from the pre-processing procedure) (Brett et al., 2002).

## GLM: Statistical Analysis

### Study 1

On a single subject level, GLM analysis was performed as follows: onset regressors of the five experimental conditions ‘double cue’, ‘spatial cue’, ‘no cue’, ‘congruent target’ and ‘incongruent target’ were implemented as regressors of interest within the statistical model. Onsets of the cue conditions ‘double cue’ and ‘spatial cue’ were defined as the time point when a cue was presented, onsets of the ‘no cue conditions’ were determined as 550 ms before target presentation (150 ms cue presentation, 400 ms cue-target interval). Onsets of target conditions were defined as the onset of target presentation. Only correct trials entered statistical analyses, onsets of error trials and six movement parameters from realignment, respectively, were added in terms of regressors of no interest. As basis set the canonical hemodynamic response function was chosen, model derivatives were not used.

Data was high-pass filtered with a default size of 120s to reduce data from physiological noise such as breathing, heart rate etc.

On the group level, we aimed to identify these regions, which were activated by the task, i.e. the Main Effect of the Attention Network Task defined as 'double cue' + 'spatial cue' + 'no cue' + 'congruent target' + 'incongruent target' > implicit baseline (contrast weights: 1 1 1 1 1). We analyzed this contrast over all subjects as well as regarding potential group differences. Therefore, we performed a one-way ANOVA model using the performance group as an independent factor (good vs. bad performers) and activation maps as the dependent variables. Activation was considered significant when $p<.05$ FDR-corrected for multiple comparisons.

## Studies 2 and 3

The factor impulsive phenotype was defined as high impulsive (highImp) versus low impulsive subjects (lowImp), based on the subjects' number of premature responses. If the number was ≥ 3 they were classified as highImp and if the number was <3 as lowImp. Threshold definition was adapted from Feja et al. (2014) in terms of the median value of premature responses across all subjects [range: 0–6 number of premature responses (adapted from Feja et al., 2014) (Feja et al., 2014)]. The sample consisted of 66 lowImp subjects and 38 highImp.

Group comparisons were performed using two sample t-tests. To correct for multiple comparisons, FDR-correction as suggested by Benjamini and Hochberg (Benjamini & Hochberg, 1995b) was applied for 17 comparisons. In addition to factorial analyses correlations were performed in order to address linear relations between impulsivity and wavelet parameters.

# Acknowledgements

This work was supported by grants from the Deutsche Forschungsgemeinschaft (DFG, German Research Foundation) – project number 44541416 – TRR 58 (project C02 to KD, project Z02 to KD and MR), the Interdisciplinary Center for Clinical Research (IZKF), University of Wuerzburg (N-262 to KD) and the Verein zur Durchführung Neurowissenschaftlicher Tagungen e.V.

# Publication List

Total publications: 14, h-index: 5, sum of times cited: 94 (without self-citations: 87), citing articles: 86 (without self-citations: 81)


Akhrif A, Romanos M, Domschke K, Schmitt-Boehrer A, Neufang S (2018). Fractal Analysis of BOLD Time Series in a Network Associated with Waiting Impulsivity. *Front Physiol.* 9:1378.

Neufang S, Geiger MJ, Homola GA; Mahr M, Schiele MS, Gehrmann A, Schmidt B, Gajewska A, Nowak J, Meisenzahl-Lechner E, Pham M, Romanos M, Ahrif A, Domschke K (ahead of print). Cognitive-behavioral therapy effects on alerting network activity and effective connectivity in panic disorder. *Eur Arch Psychiatry Clin Neurosci*.

Akhrif A, Geiger MJ, Romanos M, Domschke K, Neufang S (2017), Task Performance changes the amplitude and timing of the BOLD signal. *Transl Neurosci,* 8: 182-190.

Neufang S, Akhrif A, Hermann CG, Drepper C, Homola GA, Nowal J, Waider J, Schmitt AG, Lesch KP, Romanos M (2016). Serotonergic modulation of 'waiting impulsivity' is mediated by the impulsivity phenotype in humans. *Transl Psychiatry,* 6(11): e940.

Geiger MJ, Domschke K, Homola GA, Schulz SM, Nowak J, Akhrif A, Pauli P, Deckert J, Neufang S (2016). ADORA2A genotype modulates interoceptive and exteroceptive processing in a fronto-insular network. *Eur Neuropsychopharmacol,* 26(8): 1274-1285.

Pasquini L, Scherr M, Tahmasian M, Myers NE, Ortner M, Kurz A, Förstl H, Zimmer C, Grimmer T, Akhrif A, Wohlschläger AM, Riedl V, Sorg C (2016). Increased intrinsic activity of medial-temporal lobe subregions is associated with decreased cortical thickness of medial-parietal areas in patients with Alzheimer's disease dementia. *J Alzheimers Dis,* 51(1):313.326.

Domschke K, Akhrif A, Romanos M, Bajer C, Mainusch M, Romanos M, Winkelmann J, Zimmer C, Neufang S (2017). Neuropeptid S receptor gene variation differentially modulates frnto-limbic effective connectivity in childhood and adolescence. *Cereb Cortex,* 27(1):554-566.

Neufang S, Geiger MJ, Homola GA, Mahr M, Akhrif A, Nowak J, Reif A, Romanos M, Deckert J, Somymosi L, Domschke K (2015). Modulation of prefrontal functioning in attention systems by NPSR1 gene variation. *Neuroimage,* 114:199-206.

Neufang S, Akhrif A, Riedl V, Förstl H, Kurz A, Zimmer C, Sorg C, Wohlschläger AM (2014). Predicting Effective Connectivity from Resting-State Networks in Healthy Elderly and Patients with prodromal Alzheimer's Disease. *Human Brain Mapp,* 35(3): 954-963.

Akhrif A, Neufang S (2013). Applying Magnetic Resonance imaging to neural network connectivity. *J Neurosci Neuroeng,* 2(6): 504-516.

Akhrif A, Bajer C, Wohlschläger AM, Konrad K, Neufang S (2013). Development-related dynamics in a top-down control network. *J Neurosci Neuroeng,* 2(3): 255-266.

Akhrif A, Bajer C, Wohlschläger AM, Konrad K, Neufang S (2013). Frequency-specific top-down modulation within a fronto-parietal network- a multi-modal connectivity study. *J Neurosci Neuroeng,* 2(3): 272-279.

Mehnert J, Akhrif A, Telkemeyer S, Rossi S, Schmitz C, Steinbrink J, Wartenburger I, Obrig H, Neufang S (2012). Developmental changes in brain activation and functional connectivity during response inhibition in the early childhood brain. *Brain Dev,* 35(10):894-904.

Neufang S, Akhrif A, Riedl V, Förstl H, Kurz A, Zimmer C, Sorg C, Wohlschläger AM (2011). Disconnection of frontal and parietal areas contributes to impaired attention in very early Alzheimer's disease. J Alzheimers Dis, 2011;25(2):309-21.

# Affidavit

I hereby confirm that my thesis entitled „ The BOLD signal is more than a Brain Activation Index" is the result of my own work. I did not receive any help or support from commercial consultants. All sources and / or materials applied are listed and specified in the thesis.

Furthermore, I confirm that this thesis has not yet been submitted as part of another examination process neither in identical nor in similar form.

Würzburg,

Place, Date Signature

# Eidesstattliche Erklärung

Hiermit erkläre ich an Eides statt, die Dissertation „Das BOLD Signal ist mehr als ein Maß für Hirnaktivierung" eigenständig, d.h. insbesondere selbständig und ohne Hilfe eines kommerziellen Promotionsberaters, angefertigt und keine anderen als die von mir angegebenen Quellen und Hilfsmittel verwendet zu haben.

Ich erkläre außerdem, dass die Dissertation weder in gleicher noch in ähnlicher Form bereits in einem anderen Prüfungsverfahren vorgelegen hat.

Würzburg,

Ort, Datum Unterschrift